

# Estimating a social cost of carbon for global energy consumption

<https://doi.org/10.1038/s41586-021-03883-8>

Received: 25 February 2020

Accepted: 6 August 2021

Published online: 13 October 2021

 Check for updates

Ashwin Rode<sup>1</sup>✉, Tamma Carleton<sup>2,3</sup>, Michael Delgado<sup>4</sup>, Michael Greenstone<sup>3,5</sup>, Trevor Houser<sup>4</sup>, Solomon Hsiang<sup>3,6</sup>✉, Andrew Hultgren<sup>15</sup>, Amir Jina<sup>3,7</sup>, Robert E. Kopp<sup>8,9</sup>, Kelly E. McCusker<sup>4</sup>, Ishan Nath<sup>10</sup>, James Rising<sup>11</sup> & Jiacan Yuan<sup>12,13,14,15</sup>

Estimates of global economic damage caused by carbon dioxide (CO<sub>2</sub>) emissions can inform climate policy<sup>1–3</sup>. The social cost of carbon (SCC) quantifies these damages by characterizing how additional CO<sub>2</sub> emissions today impact future economic outcomes through altering the climate<sup>4–6</sup>. Previous estimates have suggested that large, warming-driven increases in energy expenditures could dominate the SCC<sup>7,8</sup>, but they rely on models<sup>9–11</sup> that are spatially coarse and not tightly linked to data<sup>2,3,6,7,12,13</sup>. Here we show that the release of one ton of CO<sub>2</sub> today is projected to reduce total future energy expenditures, with most estimates valued between –US\$3 and –US\$1, depending on discount rates. Our results are based on an architecture that integrates global data, econometrics and climate science to estimate local damages worldwide. Notably, we project that emerging economies in the tropics will dramatically increase electricity consumption owing to warming, which requires critical infrastructure planning. However, heating reductions in colder countries offset this increase globally. We estimate that 2099 annual global electricity consumption increases by about 4.5 exajoules (7 per cent of current global consumption) per one-degree-Celsius increase in global mean surface temperature (GMST), whereas direct consumption of other fuels declines by about 11.3 exajoules (7 per cent of current global consumption) per one-degree-Celsius increase in GMST. Our finding of net savings contradicts previous research<sup>7,8</sup>, because global data indicate that many populations will remain too poor for most of the twenty-first century to substantially increase energy consumption in response to warming. Importantly, damage estimates would differ if poorer populations were given greater weight<sup>14</sup>.

Quantifying the benefits of greenhouse gas mitigation is a topic of considerable importance to researchers and policymakers alike. The ‘social cost of carbon’ (SCC)—defined as the dollar value of climate change damages imposed globally by an additional (that is, ‘marginal’) ton of carbon dioxide (CO<sub>2</sub>) emissions (or its equivalent)—provides a means to determine the global social benefits of mitigation policies<sup>6</sup>. So far, our understanding of the SCC has been informed by theoretical-numerical integrated assessment models (IAMs)<sup>9–11</sup>. These pioneering models have produced numerous valuable insights and guided research and policy for decades<sup>15</sup>. For instance, SCC estimates derived from these models have been used by the US federal government to assess over 80 policies so far, with a combined value of US\$1 trillion in estimated benefits<sup>15</sup>. Yet as research has progressed with advances in data and computing, new challenges and opportunities have emerged<sup>3,13</sup>.

Recent assessments<sup>2,3,6,7</sup> have raised concerns that the category of current IAMs used to perform aggregate benefit–cost analyses related to climate change<sup>16</sup> are not tightly constrained by data. They also do not utilize the best-available Earth-system models, do not capture many known linkages between climate change and society, and only resolve damages at the geographic scale of large regions (for example, continents). We address these concerns by designing a fully modular ‘bottom up’ architecture, the Data-driven Spatial Climate Impact Model (DSCIM)<sup>17</sup>, to develop ‘partial’ SCC estimates for individual subsectors of the global economy (for example, agriculture, health and labour), using representative data and detailed climate models<sup>7,18–25</sup>. Each global partial SCC is built up from econometrically derived, probabilistic, local damage estimates for thousands of geographic regions. In ongoing work, we are integrating these partial SCC estimates<sup>17</sup> to compute a total SCC, taking into account intersector linkages. Previously,

<sup>1</sup>Energy Policy Institute, University of Chicago, Chicago, IL, USA. <sup>2</sup>Bren School of Environmental Science and Management, University of California, Santa Barbara, Santa Barbara, CA, USA.

<sup>3</sup>National Bureau of Economic Research, Cambridge, MA, USA. <sup>4</sup>Rhodium Group, New York, NY, USA. <sup>5</sup>Department of Economics, University of Chicago, Chicago, IL, USA. <sup>6</sup>Global Policy Laboratory, Goldman School of Public Policy, University of California, Berkeley, Berkeley, CA, USA. <sup>7</sup>Harris School of Public Policy, University of Chicago, Chicago, IL, USA. <sup>8</sup>Department of Earth & Planetary Sciences, Rutgers University, New Brunswick, NJ, USA. <sup>9</sup>Rutgers Institute of Earth, Ocean, and Atmospheric Sciences, Rutgers University, New Brunswick, NJ, USA. <sup>10</sup>Department of Economics, Princeton University, Princeton, NJ, USA. <sup>11</sup>School of Marine Science and Policy, University of Delaware, Newark, DE, USA. <sup>12</sup>Department of Atmospheric and Oceanic Sciences, Fudan University, Shanghai, China. <sup>13</sup>Institute of Atmospheric Sciences, Fudan University, Shanghai, China. <sup>14</sup>IRDR ICoE-RIG-WECEIPHE, Fudan University, Shanghai, China. <sup>15</sup>Big Data Institute for Carbon Emission and Environmental Pollution, Fudan University, Shanghai, China. ✉e-mail: aarode@uchicago.edu; shsiang@berkeley.edu

'top down' econometric results describing the gross domestic product (GDP) impacts of warming<sup>26,27</sup> have been translated into SCC values<sup>28,29</sup>; however, to our knowledge, no existing IAM transparently assembles a bottom-up and globally representative SCC based on local econometric-based projections of damage<sup>6</sup>.

## Climate-driven energy expenditures

Here we develop empirically derived estimates of the net change in global energy expenditures associated with an additional ton of CO<sub>2</sub> emissions, that is, a partial SCC for energy expenditure. IAM developers have themselves argued that the uncertainty over this number is the most important uncertainty to resolve in the total SCC<sup>8</sup>, in part because some models predict that increasing energy expenditures will be the single largest global cost from warming<sup>16</sup>. Previous econometric studies have measured the effect of local temperatures on local electricity consumption<sup>30–34</sup>, although they often omit non-electric energy consumption (for example, natural gas used for heating) because the data are difficult to obtain. Moreover, these studies generally focus on residential end uses in regions that are wealthy and thus not globally representative (for example, California). In contrast, an appealing feature of non-econometric studies using process-based models is that they simulate how climate change will affect all aspects of the production, conversion, delivery and use of energy<sup>35–38</sup>. However, similar to IAMs, their drawback is that they are not generally constrained by plausibly causal econometric estimates of consumption behaviour in response to warming. This analysis recovers globally representative measurements of total energy consumption in response to increasing temperatures, accounting for economic development and adaptive behaviour, and uses these results to compute a partial SCC for energy expenditure.

As there remains debate on how best to aggregate costs across populations over time<sup>39,40</sup> (that is, discounting), here we present results using multiple approaches and a range of parameter values<sup>6</sup>. When aggregating costs between different populations within a time period, we treat all individuals equally, consistent with guidance to US federal agencies<sup>6</sup>, although alternative approaches that upweight costs to poor populations have been proposed<sup>14</sup>.

## Computing a social cost of carbon

Our modular approach to computing partial SCC values using DSCIM has five steps, each of which can be implemented for each sector of the global economy. Here we apply these steps to compute the energy expenditure component of the SCC.

First, we match globally representative, longitudinal data on energy consumption with 0.25° × 0.25° globally harmonized historical climate data<sup>41</sup>. This represents, to our knowledge, the most comprehensive global dataset compiled on energy consumption and temperature ('Data assembly' in Methods, Supplementary Section A). Energy consumption data are derived from International Energy Agency (IEA) data files<sup>42</sup> that describe electricity and direct fuel consumption across residential, commercial, industrial and agricultural end-uses (excluding transportation) in 146 countries during 1971–2010. To make these data usable for global analysis, we harmonize data across diverse reporting systems and use econometric methods that minimize the influence of errors in record keeping ('Data assembly' in Methods, Supplementary Section A.1).

Second, we econometrically estimate the effect of historical temperature distributions on national annual per-capita energy consumption using random year-to-year variation<sup>24</sup>, and measure how this energy–temperature response differs across energy types (electricity and other fuels), income levels and climate zones<sup>17</sup>. This allows us to observe the effects of adaptive behaviours that populations undertake as they become richer<sup>31</sup> and/or are exposed to warmer climates<sup>34</sup> (for example, the adoption of air conditioning). Our approach accounts for all permanent differences between countries in energy consumption (for

example, due to geography or history) and all common trends in energy consumption (for example, due to macroeconomic fluctuations, price changes or technological innovations) to identify a plausibly causal effect<sup>30</sup> of temperature distributions on energy consumption. We then use the variation in income level and climate zone to predict how the energy–temperature relationship may change in association with these two factors ('Econometric estimation of energy–temperature responses' in Methods, Supplementary Section B).

Third, we project impacts of climate change in 24,378 globally comprehensive geographic regions (roughly the size of US counties; Extended Data Fig. 1) to 2099 (the final-year high-resolution climate simulations are available) by combining the econometric results above with a probabilistic ensemble of downscaled climate projections (Extended Data Fig. 2)<sup>43</sup> based on Coupled Model Intercomparison Project phase 5 (CMIP5) models<sup>19</sup>. When projecting these impacts, we account for how the energy–temperature response will evolve as populations become richer and exposed to warmer climates ('Projecting the impacts of climate change' in Methods). Standard socioeconomic scenarios<sup>22</sup> forecast that over 90% of the end-of-century population will still remain within the range of historical temperatures and incomes that we currently observe around the world (Extended Data Fig. 3). In isolating the impact of future climate change on energy consumption, we hold constant the current energy supply mix, an assumption that should be relaxed in future work.

Fourth, we monetize and pool the empirically derived damage estimates from the previous step and fit global energy expenditure damage functions by aggregating impacts across locations and indexing them against the global mean surface temperature anomaly (ΔGMST) expressed in each climate model realization<sup>18</sup>. These functions describe the full distribution of global damage conditional on ΔGMST. We estimate damage functions up to 2100 that evolve over time to reflect expected changes in socioeconomics and adaptation, and extrapolate their continuing evolution forward to 2300 ('Estimating global energy damage functions' in Methods, Supplementary Section D)<sup>17</sup>.

Fifth, we adapt a probabilistic, simple climate–carbon cycle model<sup>25</sup> to project the distribution of annual ΔGMST up to 2300 that results from the release of an additional 1 GtC of CO<sub>2</sub> ('Calculating the partial SCC' in Methods, Supplementary Section E). Applying the distribution of the impulse responses of ΔGMST to the damage functions from the previous step generates a probability distribution for the stream of total global damages that result from the emission of a marginal ton of CO<sub>2</sub> today. This probability distribution accounts for uncertainty in our econometric estimates at all stages of the analysis as well as climatological uncertainty. Finally, the value of the flow of damage is discounted<sup>6</sup> to capture the partial SCC for global energy expenditure.

## Energy consumption and temperature

### The role of income

Empirically, we find that a population's average income per capita is a key determinant of how its end-use energy consumption responds to temperature. Electricity–temperature responses (Fig. 1a) are U-shaped (that is, increasing with hot and cold temperatures), but only in the seventh decile or higher of the global income distribution (annual per-capita income ≥US\$11,258, 2019 purchasing power parity (PPP)), whereas the other fuels–temperature response is L-shaped (that is, increasing with cold temperatures) in the third decile or higher (annual per-capita income ≥US\$ 2,849, 2019 PPP). Above these thresholds, increasing incomes appear to amplify both responses, such that in the top decile, electricity consumption increases by 0.017 GJ per capita (4.6 kWh per capita, 66% of 2010 global average per-capita daily consumption) on a 35 °C day (relative to a 20 °C day) and by 0.0068 GJ per capita (1.9 kWh per capita, 27% of 2010 global average per-capita daily consumption) on a 0 °C day, on average, whereas direct consumption of other fuels increases by 0.034 GJ per capita (50% of 2010 global average

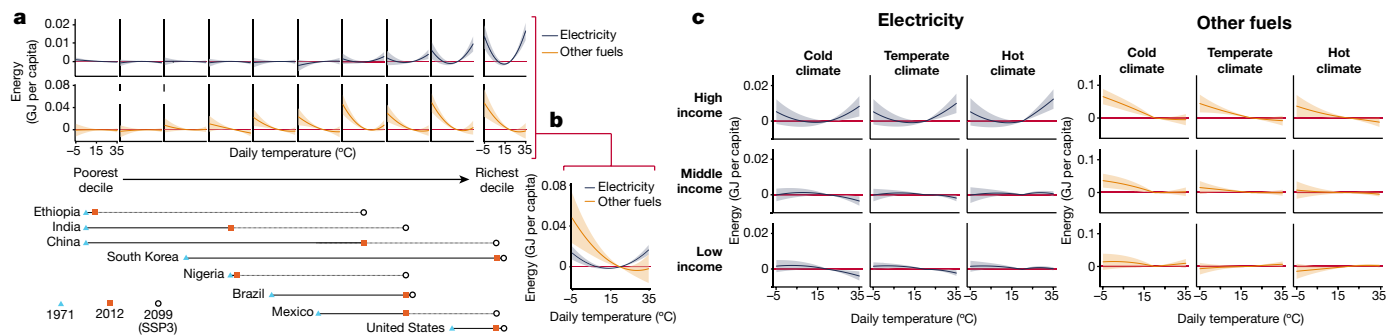


**Fig. 1 | Estimated effect of temperature on energy consumption is mediated by income and climate.** Additional daily electricity (blue) or other fuels (orange) consumption per capita (GJ per capita) in response to daily average temperature, relative to a reference temperature of 20 °C. Solid lines depict point estimates and shading is the 95% CI ( $n=7,563$ ). **a**, Separate energy–temperature relationships for global deciles of income (sample is 146 countries over 1971–2010, see Supplementary equation (B.3)), based on 15-year moving-average annual GDP per capita. Income decile boundaries are held fixed over time and incomes of selected country–years are indicated. Future income is drawn from

the SSP3 socioeconomic scenario<sup>22</sup>. **b**, Overlay of fuel-specific responses for the richest decile on a common scale. **c**, Estimated energy–temperature relationship as simultaneously influenced by income and local long-run climate (Methods, equation (3)). Each cell within a matrix illustrates a predicted energy–temperature relationship for a level of income and long-run climate. The rows separate income terciles (increasing income from bottom to top) and the columns separate climate terciles based on annual cooling degree days (increasingly warm climate from left to right; ‘Econometric estimation of energy–temperature responses’ in Methods, Supplementary Section B.3).

per-capita daily consumption) on a 0 °C day. These differing responses probably reflect the use of electricity for cooling and heating, compared with the use of other fuels (for example, natural gas, oil and coal) for heating. Previous research has documented similarly U-shaped electricity–temperature responses in the top decile<sup>30,32–34</sup> (see Supplementary Section H for comparisons), but our data reveal that such responses do not generalize to other income levels nor do they capture the substantial other fuels–temperature response, which dominates on cold days (Fig. 1b). These findings represent an empirical demonstration of how economic development shapes energy–temperature responses on a global, macroeconomic scale. The differing income thresholds at which electricity and other fuels consumption start to respond to temperature are consistent with microeconomic evidence that air conditioning is widely adopted only at very high income levels<sup>31,44</sup>, whereas solid fuels are burned for heating even in lower-income settings<sup>45,46</sup>.

### Adaptation to local long-run climate

Although income per capita is the dominant driver of the energy–temperature response, long-run climate also has a smaller role in how populations adapt. For instance, higher air-conditioning adoption in hot locations may increase electricity use on hot days<sup>31,34</sup>. We empirically recover how income and long-run climate continuously and jointly shape the energy–temperature response (Methods, equation (3), Supplementary Section B.3), thereby accounting simultaneously for the effects of economic development and climate (Fig. 1c). We find evidence that populations adapt to their long-run climate in ways that change their energy consumption during hot and cold periods, conditional on their income level. For instance, on a 35 °C day, per-capita electricity consumption is 0.004 GJ (16% of 2010 global average per-capita daily consumption) greater in the hottest climate tercile relative to the coldest. Conversely, on a 0 °C day, per-capita consumption of electricity and other fuels are 0.0002 GJ (1% of 2010 global average per-capita daily consumption) and 0.027 GJ (40% of 2010 global average per-capita daily consumption) greater, respectively, in the coldest tercile relative to the hottest. These results are consistent with populations adopting more heating or cooling technologies when their climate is cooler or hotter, respectively.

### Impacts of future climate change

#### Accounting for local adaptation globally

Combining the measured relationships estimated using country-by-year energy consumption observations (Fig. 1c) with projections for how

incomes and climate will change over the next century in each of 24,378 globally comprehensive geographic units, we project how the structure of energy–temperature responses will evolve (‘Projecting the impacts of climate change’ in Methods, Supplementary Section B.3). This spatial granularity contrasts with existing IAMs used to develop SCC estimates, which partitioned the world into at most 16 units<sup>10</sup> (Extended Data Fig. 1). Previous analysis<sup>18</sup> has demonstrated that accounting for this spatial granularity is crucial to capture the unequal impacts of climate change within countries. Applying the ensemble of downscaled climate models and surrogates (‘Data assembly’ in Methods, Supplementary Section A.2.2) to our evolving projections of local energy–temperature responses, we isolate the additional energy consumption in each region caused by changes in the temperature distribution, over and above any changes to consumption that would occur without climate change, such as those increases associated with economic development (Methods, equation (4)).

### Impacts on energy consumption

In a high-emissions scenario (representative concentration pathway (RCP) 8.5), we project that by the end of the century, most of the world is expected to increase net annual per-capita electricity consumption and decrease consumption of other fuels due to climate change (Fig. 2a). The amplitude of these effects reflects differences in incomes and climates across locations. Hot and wealthy locations show large net increases in electricity consumption, although very cold locations show net declines where warming does not increase the number of hot days enough to offset the loss of cold days. Low-income regions, such as much of sub-Saharan Africa, do not increase electricity consumption as dramatically because they are projected to still have relatively low incomes at the end of the century (for example, see Ethiopia in Fig. 1a). Declines in the consumption of other fuels are projected throughout the world, consistent with the use of these fuels for heating across a wider range of incomes.

To understand the scale of these impacts, they can be compared with current levels of energy consumption (Fig. 2b). In many of today’s rich countries, impacts at the end of the century are projected to be modest relative to current consumption, for example, a +2.7% relative increase in annual US electricity consumption. This small magnitude is due to high current consumption levels in conjunction with the fact that many rich countries are in temperate climates, where large projected increases and decreases in electricity consumption—from more hot and fewer cold days, respectively—offset one another. In contrast, in many of the poorest and/or most populous countries, the additional consumption imposed by climate change is projected to be substantial relative

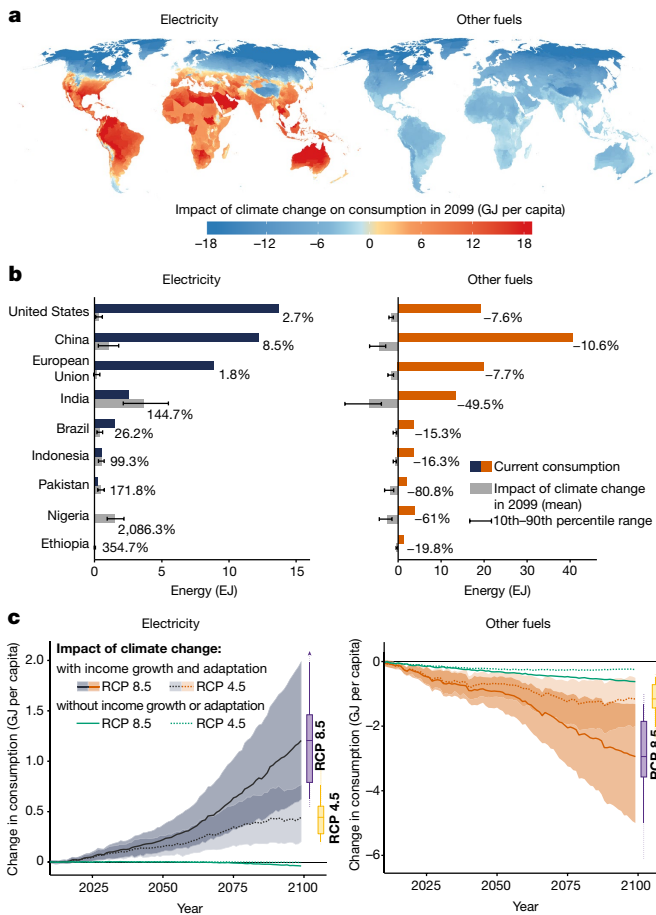


**Fig. 2 | Projected impact of climate change on energy consumption in the twenty-first century.** Projected impacts of climate change under high (RCP 8.5) or moderate (RCP 4.5) emissions scenarios (SSP3 socioeconomic scenario). **a**, The spatial distribution of projected consumption impacts across 24,378 subnational geographic regions in 2099 (RCP 8.5), accounting for the effect of income growth and adaptation on energy–temperature responses in each region. Map (produced with R software, ggplot2 package, using GADM basemap<sup>50</sup>) shows mean impacts across 33 climate models and model surrogates. **b**, Aggregating to countries, grey bars show total impacts in 2099 (RCP 8.5) alongside current consumption levels for selected countries (blue, electricity; orange, other fuels). Percentages are ratios of grey bars relative to coloured bars. Intervals indicate 10th–90th percentiles of projected distributions, accounting for climate model and econometric uncertainty (Supplementary Section B.5). **c**, Aggregating globally, time series of total global impacts. Shading indicates 10th–90th percentile range of projected distributions, accounting for climate model and econometric uncertainty. Boxplots show full distribution in 2099 (boxes, interquartile range; solid whiskers, 10th–90th percentiles; dashed whiskers, 5th–95th percentiles). The green lines illustrate projected impacts if present-day energy–temperature responses are held fixed and do not respond to increasing incomes and changing temperatures.

to current consumption, for example, a +2,000% relative increase in annual Nigerian electricity consumption. This is due both to uniformly hot temperatures and very low levels of current energy use.

Aggregating energy impacts globally, we project that in a high-emissions scenario, annual electricity consumption will increase due to climate change by 1.21 GJ per capita (90% confidence interval (CI) = [0.54, 2.43],  $P < 0.001$ ) in 2099 (RCP 8.5), whereas consumption of other fuels will decline by 2.94 GJ per capita ([1.02, 6.15],  $P < 0.01$ ) (Fig. 2c). Estimates in a moderate emissions scenario (RCP 4.5) are 0.44 GJ per capita and 1.16 GJ per capita, respectively. (Electricity impacts do not include the primary energy lost in conversion

to electricity.) It is notable that ignoring the effects of income growth and climate adaptation on the energy–temperature response would have resulted in dramatic underestimation of projected changes to global energy consumption due to warming (green lines in Fig. 2c, Supplementary Section D).

### Impacts on total energy expenditures

We monetize the climate change-induced changes in total energy consumption (electricity and other fuels combined) to develop a measure of the economic damages from climate change, that is, all economic resources that would be available for other purposes in the absence of warming. In a baseline scenario of future real energy price growth of 1.4% per year (the historical growth rate of US energy prices), we project that end-of-century warming will cause net energy expenditure declines in much of the world, although there are net increases in many tropical and subtropical middle-income regions, such as portions of India, China, Indonesia and Mexico (Fig. 3a). This pattern occurs because currently low-income countries will probably be rich enough by the end of the century to consume other fuels on cold days but not rich enough to consume electricity on hot days; thus, they experience savings from warming because it reduces other fuel costs (for example, Ethiopia in Fig. 1a). Hot middle-income countries will be rich enough to spend on electricity for cooling in the future, so in some regions, the additional spending on electricity during hot days outweighs the savings on cold days (for example, India in Fig. 1a). The largest overall savings are projected to occur among today's richest countries; however, net savings are projected across most of the present-day income distribution (Extended Data Fig. 4).

Aggregating costs globally, we project modest net savings at the end of the century due to climate change, amounting to 0.17% ( $[-0.1\%, 0.53\%]$ ,  $P < 0.3$ ) and 0.08% ( $[-0.03\%, 0.21\%]$ ,  $P < 0.25$ ) of 2099 world GDP in RCP 8.5 and RCP 4.5, respectively (Fig. 3b). The magnitude of net global savings is similar across alternative pricing scenarios (Extended Data Fig. 5, Supplementary Section C). This result differs qualitatively from the increased energy spending reported in previous studies<sup>16,18,30,32–34</sup> that focused on electricity consumption in wealthy regions. As low-income and middle-income populations spend little on electricity to cool and other fuels are consumed everywhere almost exclusively for heating, projections that use only electricity–temperature responses from high-income populations will overestimate new cooling expenditures and underestimate savings from reduced heating, leading to systematic overestimation of the total energy damages from climate change.

### Future damages from CO<sub>2</sub> emissions today

Damage functions describe the relationship between ΔGMST and global aggregate costs in a sector or the economy as a whole—they are at the centre of all IAMs used to develop SCC estimates<sup>4–11</sup>, informing mitigation policy implications by summarizing the costs of additional warming. We construct empirically based global damage functions for energy consumption using the method in refs. <sup>17,18</sup>, organizing global aggregate costs into functions of realized ΔGMST across 33,000 simulations (Fig. 3c). These damage functions evolve over time, thereby capturing the influence of changing demographics, increasing incomes and warming local climates ('Estimating global energy damage functions' in Methods). Damages are slightly quadratic in ΔGMST, although essentially linear, with an additional +1°C ΔGMST warming at the end of the century (relative to the 2001–2010 average) increasing annual consumption of electricity by an additional 4.54 EJ ([4.50, 4.59],  $P < 0.001$ ) and decreasing consumption of other fuels by 11.28 EJ ([11.12, 11.44],  $P < 0.001$ ), causing a net reduction in energy expenditures by US\$176 billion per 1°C in ΔGMST ([169, 183],  $P < 0.001$ ). Earlier and later damage functions are less and more steep, respectively, primarily due to trends in income and population (Fig. 3d, 'Estimating global energy damage functions' in Methods, Supplementary Section D).

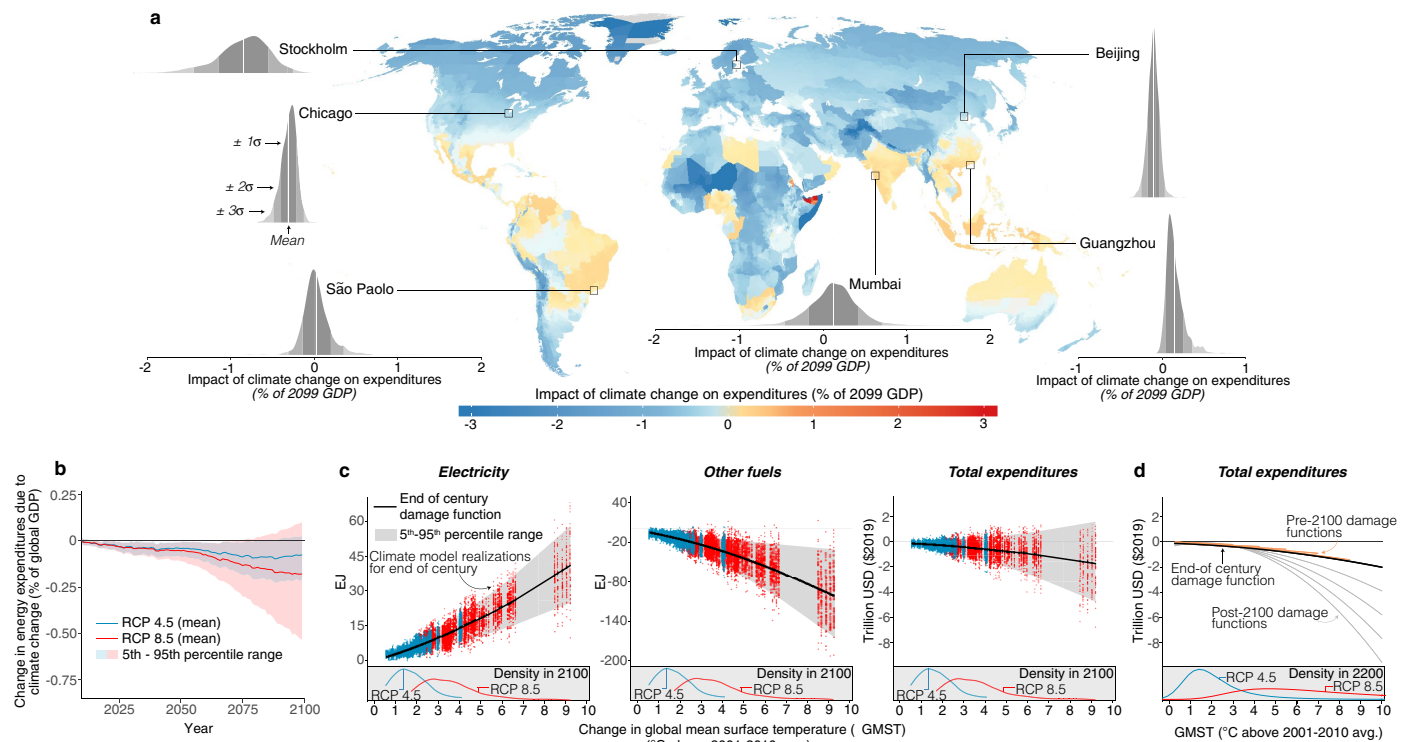


**Fig. 3 | Economic costs from energy consumption impact of climate change.** **a**, Change in 2099 total annual energy expenditures (electricity + other fuels) due to warming in a high-emissions scenario (RCP 8.5), SSP3 socioeconomic scenario and 1.4% annual price growth scenario, expressed as a percentage of 2099 local GDP for 24,378 geographic regions. The map (produced with R software, ggplot2 package, using GADM basemap<sup>50</sup>) depicts the mean; the probability density functions for selected cities plot the distribution of projected impacts accounting for climate model and econometric uncertainty (Supplementary Section B.5). **b**, Time series of globally aggregated change in total energy expenditures under both high (RCP 8.5) and moderate (RCP 4.5) emissions scenarios, expressed as a percentage of

global GDP in each year. **c**, Global energy damage functions. Total global electricity consumption impacts, other fuels consumption impacts and total energy expenditure impacts at the end of the century, indexed against  $\Delta\text{GMST}$  realized in each climate model simulation (blue dots, RCP 4.5; red dots, RCP 8.5; ‘Estimating global energy damage functions’ in Methods). The probability density functions show the distribution of  $\Delta\text{GMST}$  at the end of the century in each emissions scenario. **d**, Damage functions evolve over time. Estimated using high-resolution projections pre-2100 (for example, orange curves, every 10 years) and extrapolated post-2100 (for example, grey curves, every 50 years; Supplementary Section D).

As CO<sub>2</sub> is long lived in the atmosphere, the US National Academy of Sciences recommends computing SCC values that capture damages to the year 2300<sup>6</sup>. To do this, we combine our empirically derived damage functions with the Finite Amplitude Impulse Response (FAIR) climate model<sup>25</sup> to project to 2300 the distribution of  $\Delta\text{GMST}$  responses to the emission of a marginal 1 GtC of CO<sub>2</sub> (Supplementary Section E) (The high-resolution CMIP5 model runs used above to project spatially granular impacts end in 2100.) A CO<sub>2</sub> pulse emitted today perturbs the future trajectory of atmospheric CO<sub>2</sub> concentrations nonlinearly, affected by the half-life of CO<sub>2</sub> in the atmosphere as it is stored and released in the oceans and biosphere (Fig. 4a, b). This results in future  $\Delta\text{GMST}$  that deviates from the baseline scenario, which in turn causes a stream of energy damages in future years (Fig. 4c, d). The partial SCC from energy expenditure is the net present value (NPV) of these annual damages. As there are multiple views on how best to discount future damages into an NPV (see refs. <sup>39,40</sup>), we present multiple estimates using both constant discount rates and rates that evolve with economic growth<sup>6</sup> (‘Ramsey’ discounting<sup>47</sup>; ‘Calculating the partial SCC’ in Methods).

We find that 1 t of CO<sub>2</sub> emitted today generates a total energy expenditure burden valued at −US\$13.93 to −US\$0.69 in NPV under the high-emissions RCP 8.5 scenario and −US\$4.16 to −US\$0.76 under the moderate-emissions RCP 4.5 scenario (central estimates, 1.4% price growth scenario, Fig. 4e), with most estimates between −US\$3 and −US\$1. Our finding that the partial SCC from energy expenditure

is negative and small in magnitude is broadly robust across multiple pricing scenarios (Fig. 4e, Extended Data Tables 1, 2).

## Discussion

Our estimates make use of globally comprehensive data and empirical relationships to compute a global partial SCC for energy expenditure. This approach reveals the critical role of economic development in shaping how energy consumption patterns respond to climate change, as we find that much of the world will remain too poor in the coming decades to spend substantially on energy-intensive cooling technologies. Our approach also demonstrates the importance of accounting for non-electricity energy consumption as global populations use other fuels to cope with cold temperatures even at low income levels. Together, these two factors explain why our analysis indicates that total global energy expenditures are not likely to increase dramatically in response to warming, and why marginal emissions today may in fact produce savings in global energy expenditures.

The modest magnitude of the aggregate global impacts, however, masks substantial important shifts in projected energy consumption. Most notably, projected impacts of warming in many of today’s emerging economies may impose substantial costs and represent a large fraction of current consumption. For instance, we project that climate change will increase end-of-century electricity consumption in India by over 100% of its current consumption (Fig. 2b). Future work should

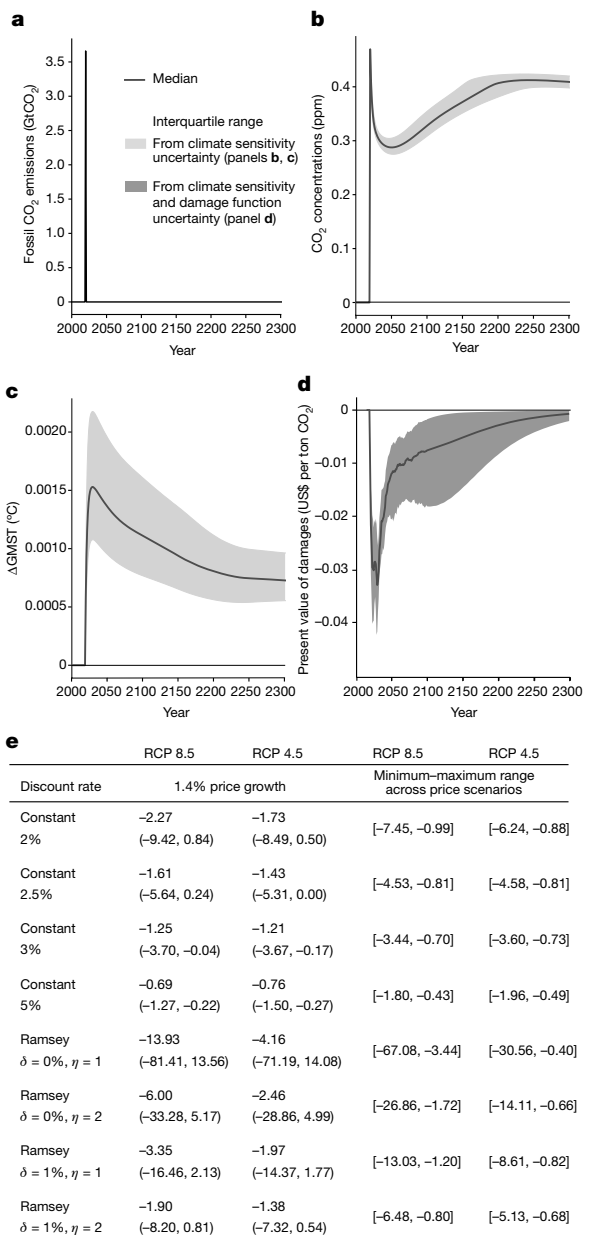


**Fig. 4 | Social cost of carbon for global energy consumption.** **a–d**, Effects of CO<sub>2</sub> pulse using the FAIR simple climate model<sup>25</sup> (RCP 8.5). The black line is the median trajectory from sampling the constrained joint distribution of climate parameters (**b,c**) and also damage function quantiles (**d**); shading indicates interquartile ranges (Supplementary Sections E.2, E.4). **a**, A1 GtC (3.66 GtCO<sub>2</sub>) pulse released in 2020. **b**, Response of atmospheric CO<sub>2</sub> concentrations, relative to baseline. **c**, Impact on ΔGMST. **d**, Change in discounted flow of energy expenditures (2% yr<sup>-1</sup> discount rate) using damage functions in Fig. 3d. The integral of this flow is the partial SCC for energy consumption. **e**, Estimates of partial SCC for energy consumption under high (RCP 8.5) and moderate (RCP 4.5) emissions scenarios. The rows apply different constant or Ramsey discount rates ( $\delta$ , pure rate of time preference;  $\eta$ , elasticity of marginal utility of consumption; ‘Calculating the partial SCC’ in Methods). ‘1.4% price growth’ assumes future energy prices reflect the historical average US price growth (1.4% yr<sup>-1</sup>). The parentheses contain 5th–95th percentile ranges, accounting for damage function and climate model uncertainty. ‘Minimum–maximum range across price scenarios’ shows the range of central estimates across alternative energy price scenarios, including those from other models (Extended Data Tables 1, 2). All estimates use socioeconomic scenario SSP3 (Supplementary Section F contains alternative scenarios).

explore alternative approaches to valuing global damages across space and time when costs are distributed unequally, as we find<sup>14</sup>.

Our approach is designed to isolate the effect of future climate change on energy consumption under given emissions and socioeconomic pathways. However, a natural area for future exploration is to account for feedback effects that climate change and climate policy may introduce via changes in the energy supply mix, the trajectory of global CO<sub>2</sub> and local air pollutant emissions, and technological innovation<sup>48,49</sup>. Although future work should explore the potential for these factors to alter the partial SCC for energy consumption, we believe at least the CO<sub>2</sub> emissions feedbacks are probably immaterial, given the small size of our aggregate estimated impacts (Extended Data Table 3).

Another extension to this analysis would be to account for additional types of future technological advancement that may affect the energy consumption response to climate change (for example, changes in the relative cost of cooling technologies). As we allow energy–temperature responses to evolve with increasing incomes and temperatures in our projection, our estimates reflect historical trends in advancement and diffusion of technology that occur with changes in these two factors. Theoretically, larger values of the partial SCC for energy consumption can arise if the price of cooling technology falls indefinitely relative to other goods and services without a corresponding trend in efficiency. However, these assumptions are unlikely to hold and we do not observe evidence of such a trend historically. The difficulty of predicting the direction and magnitude of unprecedented technological innovation under climate change underscores the critical need for further research in this area.

The results of our analysis contrast with estimates derived from alternative approaches. For example, the numerical-theoretical Climate Framework for Uncertainty, Negotiation and Distribution (FUND) IAM<sup>10</sup>—the only modelling framework where direct comparison is possible—estimates a partial SCC for energy expenditure<sup>16</sup> of US\$10 per ton of CO<sub>2</sub>, which constitutes 90% of that model’s total SCC estimate (high-emissions scenario, 3% discount rate) and is considered uncertain by its developers<sup>8</sup>. Our findings using DSCIM differ from this estimate, in part, because FUND projects very large increases in energy expenditures due to warming across many middle-income and low-income regions, such as China, North Africa, Southeast Asia and sub-Saharan Africa; in contrast, we project small or negative changes in these regions (Supplementary Section I). This divergence can be explained by the data used to inform these projections. In FUND, these regional projections are driven by parameters (for example, the income elasticity of cooling and heating energy demand) that are calibrated using data from a single high-income country (the United Kingdom)<sup>10</sup>, which we found shows energy consumption behaviour that is fundamentally different from these regions (Fig. 1a). Our findings thus underscore the importance of employing a representative empirical approach when estimating global impacts of climate change.

We demonstrate the feasibility of combining global data, econometrics, detailed climate models and modern computing within DSCIM to estimate a partial SCC for energy expenditure. Although implementing such an approach substantially reduces the energy expenditure partial SCC relative to previous estimates, this does not necessarily hold for all sectors of the economy. Although focusing on data from only wealthy locations can lead to large estimates of certain climate change damages (for example, energy expenditures), a similarly limited data focus has been shown to severely underestimate damages in other areas (for example, human health<sup>17</sup>). A total SCC, composed of many partial SCCs for different sectors of the economy, would be required to determine the full social cost of warming to global society. Our approach can be extended to the full range of outcomes potentially affected by climate (for example mortality<sup>17</sup>, agriculture and labour), thereby providing an empirically based characterization of the total SCC.

## Online content

Any methods, additional references, Nature Research reporting summaries, source data, extended data, supplementary information, acknowledgements, peer review information; details of author contributions and competing interests; and statements of data and code availability are available at <https://doi.org/10.1038/s41586-021-03883-8>.

1. Interagency Working Group on Socio Cost of Carbon Social Cost of Carbon for Regulatory Impact Analysis—under Executive Order 12866 Technical Report (United States Government, 2010).
2. Revesz, R. L. et al. Global warming: improve economic models of climate change. *Nature* **508**, 173–175 (2014).
3. Pizer, W. et al. Using and improving the social cost of carbon. *Science* **346**, 1189–1190 (2014).
4. Nordhaus, W. D. An optimal transition path for controlling greenhouse gases. *Science* **258**, 1315–1319 (1992).
5. Greenstone, M., Kopits, E. & Wolverton, A. Developing a social cost of carbon for US regulatory analysis: a methodology and interpretation. *Rev. Environ. Econ. Policy* **7**, 23–46 (2013).
6. National Academies of Sciences, Engineering, and Medicine *Valuing Climate Damages: Updating Estimation of the Social Cost of Carbon Dioxide* (The National Academies Press, 2017).
7. Diaz, D. & Moore, F. Quantifying the economic risks of climate change. *Nat. Clim. Change* **7**, 774–782 (2017).
8. Anthoff, D. & Tol, R. S. The uncertainty about the social cost of carbon: a decomposition analysis using FUND. *Climatic Change* **117**, 515–530 (2013).
9. Stern, N. *Stern Review Report on the Economics of Climate Change* (HM Treasury, 2006).
10. Waldhoff, S., Anthoff, D., Rose, S. & Tol, R. S. The marginal damage costs of different greenhouse gases: an application of FUND. *Economics* **8**, 1–33 (2014).
11. Nordhaus, W. D. *Estimates of the Social Cost of Carbon: Background and Results from the Rice-2011 Model Technical Report* (National Bureau of Economic Research, 2011).
12. Pindyck, R. S. Climate change policy: what do the models tell us? *J. Econ. Lit.* **51**, 860–872 (2013).
13. Burke, M. et al. Opportunities for advances in climate change economics. *Science* **352**, 292–293 (2016).
14. Adler, M. et al. Priority for the worse-off and the social cost of carbon. *Nat. Clim. Change* **7**, 443–449 (2017).
15. Moore, F. C., Baldos, U., Hertel, T. & Diaz, D. New science of climate change impacts on agriculture implies higher social cost of carbon. *Nat. Commun.* **8**, 1607 (2017).
16. Diaz, D. B. *Evaluating the Key Drivers of the US Government's Social Cost of Carbon: A Model Diagnostic and Inter-Comparison Study of Climate Impacts in DICE, FUND, and PAGE* (Stanford University Policy and Economics Research Roundtable, 2014).
17. Carleton, T. A. et al. *Valuing the Global Mortality Consequences of Climate Change Accounting for Adaptation Costs and Benefits Working Paper 27599* (National Bureau of Economic Research, 2020); <http://www.nber.org/papers/w27599>
18. Hsiang, S. et al. Estimating economic damage from climate change in the United States. *Science* **356**, 1362–1369 (2017).
19. Taylor, K. E., Stouffer, R. J. & Meehl, G. A. An overview of CMIP5 and the experiment design. *Bull. Am. Meteorol. Soc.* **93**, 485–498 (2012).
20. Auffhammer, M., Hsiang, S. M., Schlenker, W. & Sobel, A. Using weather data and climate model output in economic analyses of climate change. *Rev. Environ. Econ. Policy* **7**, 181–198 (2013).
21. Kopp, R., Hsiang, S. & Oppenheimer, M. Empirically calibrating damage functions and considering stochasticity when integrated assessment models are used as decision tools. In *Impacts World 2013 Conference Proc.* 834–843 (Potsdam Institute for Climate Impact Research, 2013).
22. O'Neill, B. C. et al. A new scenario framework for climate change research: the concept of shared socioeconomic pathways. *Climatic Change* **122**, 387–400 (2014).
23. Rasmussen, D. J. & Kopp, R. E. in *Economic Risks of Climate Change: An American Prospectus* 219–248 (Columbia Univ. Press, 2015); <https://cup.columbia.edu/book/economic-risks-of-climate-change/9780231174565>
24. Hsiang, S. Climate econometrics. *Annu. Rev. Resour. Econ.* **8**, 43–75 (2016).
25. Smith, C. J. et al. FAIR v1. 3: a simple emissions-based impulse response and carbon cycle model. *Geosci. Model Dev.* **11**, 2273–2297 (2018).
26. Dell, M., Jones, B. F. & Olken, B. A. Temperature shocks and economic growth: evidence from the last half century. *Am. Econ. J. Macroecon.* **4**, 66–95 (2012).
27. Burke, M., Hsiang, S. M. & Miguel, E. Global non-linear effect of temperature on economic production. *Nature* **527**, 235–239 (2015).
28. Moore, F. C. & Diaz, D. B. Temperature impacts on economic growth warrant stringent mitigation policy. *Nat. Clim. Change* **5**, 127–131 (2015).
29. Ricke, K., Drouet, L., Caldeira, K. & Tavoni, M. Country-level social cost of carbon. *Nat. Clim. Change* **8**, 895–900 (2018).
30. Deschênes, O. & Greenstone, M. Climate change, mortality, and adaptation: evidence from annual fluctuations in weather in the US. *Am. Econ. J. Appl. Econ.* **3**, 152–185 (2011).
31. Davis, L. W. & Gertler, P. J. Contribution of air conditioning adoption to future energy use under global warming. *Proc. Natl. Acad. Sci. USA* **112**, 5962–5967 (2015).
32. Auffhammer, M., Baylis, P. & Hausman, C. H. Climate change is projected to have severe impacts on the frequency and intensity of peak electricity demand across the United States. *Proc. Natl. Acad. Sci. USA* **114**, 1886–1891 (2017).
33. Wenz, L., Levermann, A. & Auffhammer, M. North–south polarization of European electricity consumption under future warming. *Proc. Natl. Acad. Sci. USA* **114**, E7910–E7918 (2017).
34. Auffhammer, M. *Climate Adaptive Response Estimation: Short and Long Run Impacts of Climate Change on Residential Electricity and Natural Gas Consumption using Big Data Technical Report* (National Bureau of Economic Research, 2018).
35. Hadley, S. W., Erickson, D. J., Hernandez, J. L., Broniak, C. T. & Blasing, T. Responses of energy use to climate change: a climate modeling study. *Geophys. Res. Lett.* **33**, L17703 (2006).
36. Zhou, Y., Eom, J. & Clarke, L. The effect of global climate change, population distribution, and climate mitigation on building energy use in the US and China. *Climatic Change* **119**, 979–992 (2013).
37. Isaac, M. & Van Vuuren, D. P. Modeling global residential sector energy demand for heating and air conditioning in the context of climate change. *Energy Policy* **37**, 507–521 (2009).
38. Clarke, L. et al. Effects of long-term climate change on global building energy expenditures. *Energy Econ.* **72**, 667–677 (2018).
39. Gollier, C. & Hammitt, J. K. The long-run discount rate controversy. *Annu. Rev. Resour. Econ.* **6**, 273–295 (2014).
40. Bauer, M. & Rudebusch, G. D. *The Rising Cost of Climate Change: Evidence from the Bond Market* (Federal Reserve Bank of San Francisco, 2020).
41. Sheffield, J., Goteti, G. & Wood, E. F. Development of a 50-year high-resolution global dataset of meteorological forcings for land surface modeling. *J. Clim.* **19**, 3088–3111 (2006).
42. *World Energy Balances (Edition 2017)* International Energy Agency, 2018; <https://www.oecd-ilibrary.org/content/data/9dddec1c1-en>
43. Rasmussen, D. J., Meinshausen, M. & Kopp, R. E. Probability-weighted ensembles of US county-level climate projections for climate risk analysis. *J. Appl. Meteorol. Climatol.* **55**, 2301–2322 (2016).
44. McNeil, M. A. & Letschert, V. E. Modeling diffusion of electrical appliances in the residential sector. *Energy Build.* **42**, 783–790 (2010).
45. Legros, G. et al. *The Energy Access Situation in Developing Countries: A Review Focusing on the Least Developed Countries and Sub-Saharan Africa* (World Health Organization, 2009).
46. Almond, D., Chen, Y., Greenstone, M. & Li, H. Winter heating or clean air? Unintended impacts of China's Huai River policy. *Am. Econ. Rev.* **99**, 184–190 (2009).
47. Ramsey, F. P. A mathematical theory of saving. *Econ. J.* **38**, 543–559 (1928).
48. Tong, D. et al. Committed emissions from existing energy infrastructure jeopardize 1.5 °C climate target. *Nature* **572**, 373–377 (2019).
49. Woodard, D. L., Davis, S. J. & Randerson, J. T. Economic carbon cycle feedbacks may offset additional warming from natural feedbacks. *Proc. Natl. Acad. Sci. USA* **116**, 759–764 (2019).
50. Global Administrative Areas GADM Database of Global Administrative Areas, Version 2.0 (University of California, Berkeley, Museum of Vertebrate Zoology, International Rice Research Institute, University of California, Davis, 2012); [www.gadm.org/data.html](http://www.gadm.org/data.html)

**Publisher's note** Springer Nature remains neutral with regard to jurisdictional claims in published maps and institutional affiliations.

© The Author(s), under exclusive licence to Springer Nature Limited 2021

## Methods

Here we provide an overview of the data and methods used to complete each of the five stages of analysis that compose DSCIM, our modular approach to constructing a partial SCC. Details on each stage can be found in Supplementary Information.

### Data assembly

In the first step, we compile a comprehensive dataset on historical energy consumption, climate and income, as well as future projections of climate, income, populations and energy prices (Supplementary Section A). Historical data are used to econometrically estimate the energy–temperature response, and how it differs by energy type (electricity and other fuels), income and climate. Future projection data are used to generate high-resolution projected impacts of climate change, accounting for the effects of income growth and warming on the shape of the energy–temperature response.

**Historical datasets.** Annual data on final consumption of electricity and other fuels for 146 countries from 1971 to 2010 were obtained from the IEA's World Energy Balances dataset<sup>42</sup>. We take electricity consumption directly from the dataset, whereas other fuels consumption is constructed by aggregating over coal, peat, oil shale and oil sands, oil products, natural gas, solar, wind, geothermal, biofuels and waste, heat, and heat production from non-specified combustible fuels. For both electricity and other fuels, we aggregate over the industrial, commercial/public services, residential, agricultural, forestry, fishing and non-specified sectors. Data inconsistencies and quality issues in the IEA's records are extensively documented<sup>42</sup>. We classify every such change in record-keeping methodology and employ specific data preparation and econometric techniques to address each individually (Supplementary Section A.1).

Historical data on daily average temperature and precipitation, as well as historical climatologies, are obtained from the Global Meteorological Forcing Dataset, v1 (GMFD)<sup>41</sup>, a global gridded ( $0.25^\circ \times 0.25^\circ$ ) daily climate record available from 1948 to 2010<sup>20</sup>. We link high-resolution daily climate data to country-level annual energy consumption data using a procedure detailed in Supplementary Section A.2.4 that preserves nonlinearity in the energy consumption response to daily temperature.

We obtain historical values of country-level annual income per capita (constant dollar PPP) from within the IEA's World Energy Balances dataset, which in turn sources these data from the World Bank.

**Datasets of future projections.** We use a set of 21 high-resolution ( $0.25^\circ \times 0.25^\circ$ ) bias-corrected global climate projections that provide daily temperature and precipitation to the year 2099 from the NASA Earth Exchange (NEX) Global Daily Downscaled Projections (GDDP) dataset<sup>51</sup>. We obtain climate projections based on two standardized emissions scenarios: RCP 4.5 (an emissions stabilization scenario) and RCP 8.5 (a scenario with intensive growth in fossil fuel emissions)<sup>52–54</sup>. As this set of 21 climate models systematically underestimates tail risks of future climate change<sup>43,55</sup>, we assign probabilistic weights to climate projections and use 12 surrogate models that describe local climate outcomes in the tails of the climate-sensitivity distribution<sup>43</sup>. The 21 models and 12 surrogate models are treated identically in our calculations and are referred to as the surrogate/model mixed ensemble (SMME). We utilize the probabilistic weights when calculating and reporting summary statistics of impact estimates across the 33 models and surrogates (Extended Data Fig. 2, Supplementary Section B.5). Full details on the SMME climate projections are in Supplementary Section A.2.3. The gridded output from these projections is aggregated to 24,378 globally comprehensive agglomerated political units that we call impact regions using the same method applied to historical climate data (Supplementary Section A.2.4). Impact regions are constructed to

(1) respect national borders, (2) be roughly equal in population across regions and (3) have approximately homogenous within-region climatic conditions (Extended Data Fig. 1).

Projections of national populations and income per capita are derived from the shared socioeconomic pathways (SSPs)<sup>56</sup>, a set of scenarios of socioeconomic development over the twenty-first century in the absence of climate impacts. We utilize population<sup>57</sup> and country-level GDP<sup>58,59</sup> projections for scenarios SSP1, SSP2, SSP3, SSP4 and SSP5<sup>60</sup>. These projections have been used as inputs to IAM-based projections of other social and economic outcomes, such as land-cover changes or air pollution, through the SSP research programme<sup>56</sup>, although we do not utilize these outputs in our main calculations. However, we do examine the sensitivity of our results to assuming alternative energy price projections that are output from these IAM exercises. National population projections are respectively allocated to 24,378 impact regions based on current satellite-based within-country population distributions<sup>61</sup> (Supplementary Section A.3.3) or an alternative, time-varying scenario of within-country population distributions that reflects projected urbanization<sup>62,63</sup> (Supplementary Section G.1).

The price trajectories we use to monetize estimated impacts of climate change are constructed based on either of two distinct data sources—present-day statistics from the IEA are used for our main estimates and price projections from IAMs are used in the sensitivity tests. We obtain present-day average electricity generation costs by region of the world from the IEA's World Energy Outlook 2017 (Figure 6.25); prices for other fuels are obtained from the IEA's Energy Prices and Taxes Statistics dataset. Price projections of electricity and other fuels' prices from five IAMs were obtained from the International Institute for Applied Systems Analysis (IIASA) Scenario Explorer database<sup>64</sup>. Price projections from IAMs are used only to examine the sensitivity of our results to alternative pricing assumptions; however, we note that they are derived using models that express market equilibria different from the projected changes in energy consumption that we estimate here. Details on how prices are assigned across countries and over time can be found in Supplementary Section C.

### Econometric estimation of energy–temperature responses

In the second step, we use historical data on national annual per-capita energy consumption, climate and income to flexibly model electricity and other fuels consumption each as a function of daily average temperatures within a year, while accounting for heterogeneity in energy–temperature responses along the dimensions of both income and long-run climate. Importantly, our econometric procedure is designed to recover nonlinear changes in local per-capita energy consumption at the grid-cell-by-day level, in response to locally experienced daily temperatures and these other factors. Accounting for such local nonlinearity is crucial in this context, as different locations within a country on the same day, or the same location on different days within a year, may show very different temperatures, which generate divergent energy consumption responses.

We apply methods from previous research that has demonstrated that the local effect of climate variables on many outcomes (including energy consumption) may be nonlinear in important ways<sup>65</sup>. These outcome variables are sometimes measured at the same temporal and spatial resolution as that at which these nonlinear effects manifest (for example, refs. <sup>66,67</sup>). However, in most contexts, nonlinear effects emerge over timescales and spatial scales (for example, for individual grid cells on single days) that are much finer than the scale at which outcome data are available<sup>24,30,68</sup> (for example, for entire countries over a year). Yet, despite only observing spatially and temporally aggregated outcomes (that is, annual national per-capita energy consumption), it is possible to empirically recover the nonlinear relationships that take place at the spatial and temporal scale at which the climate

# Article

variables are recorded (that is, the effect of daily grid-cell temperature on daily grid-cell per-capita energy consumption), provided that the climate variables are themselves aggregated in a way that preserves nonlinearities<sup>24,68</sup>.

Recovering such high-resolution energy consumption–temperature responses is only possible because we observe the temperature on each day in each grid cell. Conceptually, these data enable us to search for the grid-cell-level energy–temperature consumption relationship that, if applied to every grid cell for every daily temperature, would generate predicted per-capita energy consumption at the country-by-year level that best matches observed consumption. This approach is established in the broader literature; for example, ref. <sup>68</sup> estimates nonlinear local effects of daily temperature on crop yields using annual aggregate yields, and the approach is derived in the review by ref. <sup>24</sup>. Here we implement this approach through a country–year-level regression of per-capita energy consumption on specific population-weighted nonlinear climate variables (described below). A crucial step in implementation is properly constructing weighted aggregates of nonlinear transformations of local daily temperature (Supplementary Section A.2.4).

Specifically, let  $E_{zjdtc}$  denote consumption in GJ per capita in grid cell  $z$  of country  $j$ , on day  $d$  of year  $t$ , for fuel category  $c$  (electricity, other fuels), and let  $T_{zjdt}$  denote the daily average temperature at grid cell  $z$  on day  $d$ . Let  $\mathbf{T}_{zjdt}$  denote an  $M$ -element vector in which each element ( $T_{zjdt1}, \dots, T_{zjdtM}$ ) is a nonlinear transformation of grid-cell-level daily temperature (for example, polynomial terms,  $T_{zjdt1} = T_{zjdt}^1$ ,  $T_{zjdt2} = T_{zjdt}^2$ ). We assume per-capita fuel category  $c$  energy consumption at grid cell  $z$  on day  $d$  is a function of the grid cell's temperature on that day, where this function,  $f_c(\mathbf{T}_{zjdt})$ , is a linear combination of the nonlinear elements in  $\mathbf{T}_{zjdt}$ :

$$E_{zjdtc} = f_c(\mathbf{T}_{zjdt}) = \beta_{c1} T_{zjdt1} + \dots + \beta_{cM} T_{zjdtM} = \sum_{m=1}^M \beta_{cm} T_{zjdtm}, \quad (1)$$

where  $\beta_{c1}, \dots, \beta_{cM}$  are assumed to be constant average coefficients.

Daily grid-cell-level per-capita energy consumption ( $E_{zjdtc}$ ) is unavailable to us, but we observe national annual per-capita energy consumption ( $E_{jtc}$ ), which is the population-weighted average of daily per capita consumption across grid cells in the country, summed over days in the year<sup>24</sup>. Let  $w_z$  denote the share of a country  $j$ 's population that falls into grid cell  $z$ . Country  $j$ 's per-capita annual consumption in the year  $t$  is thus the weighted average of daily per capita consumption across grid cells in  $j$ , aggregated over all 365 days  $d$  in year  $t$ :

$$\begin{aligned} E_{jtc} &= \sum_{d \in t} \sum_{z \in j} w_z E_{zjdtc} = \sum_{d \in t} \sum_{z \in j} w_z \left[ \sum_{m=1}^M \beta_{cm} T_{zjdtm} \right] \\ &= \sum_{m=1}^M \beta_{cm} \left[ \sum_{d \in t} \sum_{z \in j} w_z T_{zjdtm} \right]. \end{aligned} \quad (2)$$

$\underbrace{\phantom{\sum_{d \in t} \sum_{z \in j} w_z T_{zjdtm}}}_{f_c(\tilde{\mathbf{T}}_{jt})}$

The second line of equation (2) is obtained by substitution from equation (1) and interchanging the order of summation, expressing national annual per-capita energy consumption as  $f_c(\tilde{\mathbf{T}}_{jt})$ , where  $\tilde{\mathbf{T}}_{jt}$  is an  $M$ -element vector in which the  $m$ th element,  $\tilde{T}_{jtm}$ , is a country-by-year aggregation of the corresponding element from the grid-cell-level daily vector  $\mathbf{T}_{zjdt}$  (Supplementary Section A.2.4). Removing the coefficients  $\beta_{c1}, \dots, \beta_{cM}$  from the summation over grid cells and days is possible given that these coefficients are assumed homogenous within a country and year. Thus, a regression of country-level annual per-capita energy consumption ( $E_{jtc}$ ) on variables that are country–year weighted aggregates of the nonlinear temperature terms ( $\tilde{T}_{jt1}, \dots, \tilde{T}_{jtM}$ ) recovers the same coefficients,  $\beta_{c1}, \dots, \beta_{cM}$ , that describe the primitive grid

cell-by-day relationship described by equation (1). (See Extended Data Fig. 6 for a simplified, graphical illustration of this concept.)

In practice, we allow energy–temperature responses to vary by income and long-run climate, estimating the function  $f_c(\cdot)$  conditional on these covariates. If this conditional function is homogenous within a country and year, then we can recover a grid cell-by-day relationship, as demonstrated above. To model heterogeneity by income, we use the 15-year moving average of a country  $j$ 's natural log of per-capita GDP in year  $t$  ( $\log \overline{\text{GDP}} \bar{P}_{jt}$ ). To model heterogeneity by long-run climate, we use average annual cooling degree days and heating degree days over the sample period ( $\overline{\text{CDD}_j}$  and  $\overline{\text{HDD}_j}$ , respectively). Annual cooling (heating) degree days are a common measure of exposure to warm (cold) temperatures and are defined as the cumulative deviations of daily average temperatures from a benchmark of 20 °C, over all days in the year where the average temperature exceeded (fell below) 20 °C. As these measures do not change substantially over the historical record, we do not rely on long-run temporal variation within the timespan of the sample and instead use the average over the sample period (Supplementary Section B.3).

Our estimating equation takes the following form:

$$E_{jtc} = f_c(\tilde{\mathbf{T}}_{jt} | \log \overline{\text{GDP}} \bar{P}_{jt}, \overline{\text{CDD}_j}, \overline{\text{HDD}_j}) + g_c(\tilde{\mathbf{P}}_{jt}) + \alpha_{jic} + \delta_{wct} + \varepsilon_{jtc}. \quad (3)$$

In our main specifications,  $\tilde{\mathbf{T}}_{jt}$  contains linear and quadratic terms for a spline in daily average temperatures (allowing a kink at 20 °C), each averaged over grid cells and summed across the year, as shown in equation (2). Exploiting flexible interactions between the three income and long-run climate covariates ( $\log \overline{\text{GDP}} \bar{P}_{jt}, \overline{\text{CDD}_j}$  and  $\overline{\text{HDD}_j}$ ) and all terms in the temperature vector ( $\tilde{\mathbf{T}}_{jt}$ ), we estimate an energy–temperature response  $f_c$  for fuel category  $c$  that is conditional on income and long-run climate. Details of this procedure can be found in Supplementary Section B.3. Importantly, the interactions involving the long-run climate covariates are country-by-year aggregations of grid-cell-level interactions, allowing us to recover heterogeneity in the energy–temperature response due to long-run climate at the grid-cell level. In contrast, because our income data are available only at the country level, we recover heterogeneity in the energy–temperature response due to income only at the country level.

All our econometric specifications control for the effects of precipitation through the function  $g_c(\cdot)$ , constructed analogously to  $f_c(\cdot)$ ; the vector  $\tilde{\mathbf{P}}_{jt}$  contains linear and quadratic terms of daily cumulative precipitation, each averaged over grid cells and summed annually. We also include a full set of country-by-reporting regime intercepts, referred to here as 'fixed effects' ( $\alpha_{jic}$ ), where reporting regimes ( $i$ ) are time spans within a country where observations for a given fuel category are documented by the IEA to be comparable (Supplementary Section A.1). These fixed effects flexibly account for all permanent differences in energy consumption across country regimes. In addition, we include world region-by-year fixed effects ( $\delta_{wct}$ ) for each fuel category, where  $w$  indexes world regions based on United Nations classifications (Oceania, N. America, N. Europe, S. Europe, W. Europe, E. Europe, E. Asia, S.E. Asia, Central America/Caribbean, South America, sub-Saharan Africa, N. Africa/W. Asia, S. Asia). These fixed effects flexibly account for all world region-level trends and shocks in energy consumption. The use of fixed effects is more reliable than trying to individually control explicitly for determinants of energy consumption because it accounts for time-invariant and time-trending factors non-parametrically. We thus exploit random within-country-regime, year-to-year variation in realized daily temperatures to identify a plausibly causal effect of historical temperature distributions on energy consumption, and we use variation in income and long-run climate to predict how the energy–temperature relationship may change in association with these two factors (Supplementary Section B.3). It should be noted that because our long-run climate measures ( $\overline{\text{CDD}_j}$  and  $\overline{\text{HDD}_j}$ )

do not vary over time within a country, their direct effect on energy consumption is absorbed in the fixed effects  $\alpha_{jic}$ . However, our objects of interest in equation (3) are the interactions of income and long-run climate with temperature, and not their direct effect on the level of energy consumption. Finally,  $\varepsilon_{jtc}$  denotes the stochastic error term.

Owing to evidence of unit root behaviour in the dependent variable, we estimate equation (3) in first differences (Supplementary Section A.1). Furthermore, we employ inverse variance weighting to address differences in data quality across reporting regimes (Supplementary Section B.1). Standard errors are clustered by country–fuel category–reporting regime.

Although equation (3) is designed to causally identify the effect of daily temperatures on per-capita energy consumption, it does not identify overall levels of per-capita energy consumption as these are absorbed in the spatial and temporal fixed effects. We therefore express estimated electricity–temperature or other fuels–temperature responses as predicted consumption relative to a ‘mild’ day with an average temperature of 20 °C. The matrices of electricity–temperature and other fuels–temperature responses in Fig. 1c summarize the results from estimating equation (3), whereas Fig. 1a, b displays responses that are estimated for each decile of the in-sample income distribution, but do not differ by long-run climate (Supplementary Section B.2).

### Projecting the impacts of climate change

In the third step, we estimate future per-capita energy consumption impacts of climate change. We first use estimates from equation (3) along with observable characteristics ( $\log\text{GDPPC}$ ,  $\overline{\text{CDD}}$  and  $\overline{\text{HDD}}$ ) to predict energy–temperature responses at different points in time for each of 24,378 impact regions. For each impact region  $r$  in country  $j$  at year  $t$ , we use the estimated function  $\hat{f}_c(\cdot)$  from equation (3), along with 15-year moving averages of the covariates ( $\log\overline{\text{GDPPC}}_{jt}$ ,  $\overline{\text{CDD}}_{jt}$  and  $\overline{\text{HDD}}_{jt}$ ), to predict energy–temperature responses for each fuel category. Responses evolve over time as 15-year moving averages of the covariates change for a given impact region  $r$  in country  $j$ , thereby reflecting the effects of adaptive behaviours that populations undertake as they become richer and/or are exposed to warmer climates. Because equation (3) estimates the interaction between temperature and country-level income as well as the interaction between temperature and grid-cell-level climate, our projections reflect changes in income and climate at these two corresponding spatial scales for internal consistency (Supplementary Section B.3).

We then apply a set of probabilistic climate change projections to the spatially and temporally heterogeneous energy–temperature responses to compute per-capita consumption impacts for each fuel category  $c$  and impact region  $r$  in country  $j$  for each year from 2015 to 2099. The distribution of future daily average temperatures under a given emissions scenario (RCP 8.5 or RCP 4.5) is obtained from the 33 projections in the SMME (Supplementary Section A.2.3).

Let  $\tilde{\mathbf{T}}_{rjt}$  represent a vector containing impact region-by-year aggregations of nonlinear grid-cell-level transformations of daily temperature in a future year  $t$ , under a warmer climate. In contrast, let  $\tilde{\mathbf{T}}_{rjt_0}$  represent the counterfactual temperature vector for the same impact region under a climatology that is the same as that of a historical baseline period  $t_0$  (Supplementary Section B.4). These vectors are constructed in exactly the same way as for the temperature vectors used in estimating equation (3), except that we take a weighted aggregation only over grid cells  $z$  within the impact region rather than the entire country; for example, element  $m$  of  $\tilde{\mathbf{T}}_{rjt}$  is  $\tilde{T}_{rjtm} = \sum_{d \in t} \sum_{z \in r} w_{zr} T_{zjdtm}$ , where  $w_{zr}$  denotes the share of an impact region  $r$ 's population that falls into grid cell  $z$  (Supplementary Section A.2.4). The impact of climate change on fuel category  $c$  is expressed as the estimated change in per-capita consumption relative

to a no-climate-change counterfactual in which the future climatology is the same as in  $t_0$ :

$$\begin{aligned} & \text{Impact of climate change per capita}_{crjt} \\ &= \underbrace{\hat{f}_c(\tilde{\mathbf{T}}_{rjt} | \log\overline{\text{GDPPC}}_{jt}, \overline{\text{CDD}}_{jt}, \overline{\text{HDD}}_{jt})}_{\text{Temperature-induced per-capita energy consumption under climate change (within income growth and climate-driven adaptation) (A)}} \\ &\quad - \underbrace{\hat{f}_c(\tilde{\mathbf{T}}_{rjt_0} | \log\overline{\text{GDPPC}}_{jt}, \overline{\text{CDD}}_{rjt_0}, \overline{\text{HDD}}_{rjt_0})}_{\text{Temperature-induced per-capita energy consumption without climate change (with income growth) (B)}} \end{aligned} \quad (4)$$

The object  $\text{Impact of climate change per capita}_{crjt}$  in equation (4) represents the change in annual per-capita electricity or other fuels consumption due to a shift in the temperature distribution under climate change, accounting for the evolution of energy–temperature responses as locations warm and incomes increase. It isolates the additional impact of climate change net of other factors (for example, income) that will change in the future. The two projections (A) and (B) are identical in every way, except for the climate. Thus, we evaluate (B) using future levels of income but use  $\tilde{\mathbf{T}}$ ,  $\overline{\text{CDD}}$  and  $\overline{\text{HDD}}$  values from a historical baseline  $t_0$  (Supplementary Section B.4). All fixed effects and other controls cancel out and are therefore omitted.

We construct estimates of equation (4) for all impact regions up to 2099 under emissions scenarios RCP 8.5 and RCP 4.5, using each of the 33 climate projections in the SMME. Figure 2a maps mean impact estimates across these 33 climate projections at year 2099 under RCP 8.5, whereas Fig. 2b, c shows impacts aggregated to the country and global levels, respectively. Confidence intervals around the means are constructed to reflect both climatological and econometric sources of uncertainty. The distribution of impacts across 33 climate projections captures uncertainties in the climate system to 2099, and we additionally capture uncertainty arising from econometric estimation of equation (3) using the delta method<sup>69</sup>. Supplementary Section B.5 details the method used to combine both these independent sources of uncertainty.

To highlight the critical importance of income growth and climate-driven adaptation in shaping future energy–temperature responses, we also consider a ‘no adaptation’ impact projection that ignores these factors (green lines in Fig. 2c). To do this, we project

$$\begin{aligned} & \text{Impact of climate change per capita}_{crjt}^{\text{No adaptation}} \\ &= \underbrace{\hat{f}_c(\tilde{\mathbf{T}}_{rjt} | \log\overline{\text{GDPPC}}_{jt_0}, \overline{\text{CDD}}_{rjt_0}, \overline{\text{HDD}}_{rjt_0})}_{\text{Temperature-induced per-capita energy consumption under climate change (no adaptation)}} \\ &\quad - \underbrace{\hat{f}_c(\tilde{\mathbf{T}}_{rjt_0} | \log\overline{\text{GDPPC}}_{jt_0}, \overline{\text{CDD}}_{rjt_0}, \overline{\text{HDD}}_{rjt_0})}_{\text{Temperature-induced per-capita energy consumption without climate change (no adaptation)}} \end{aligned}$$

which captures the change in consumption responses due to future temperature, holding each impact region's income and climate fixed at historical baseline values for all years in the projection.

### Estimating global energy damage functions

Our fourth step is to pool empirical estimates of climate change impacts constructed using equation (4) to fit global energy damage functions, which express global energy consumption costs of climate change as a function of the change in global mean surface temperature relative to the 2001–2010 average level ( $\Delta\text{GMST}$ )<sup>4</sup>. These damage functions summarize the economic costs of all impacts measured in the detailed empirical analysis, demonstrating how they vary with the change in global mean surface temperature.

# Article

Damages functions to 2099 are directly built from estimates of global costs ( $D_{t,ps}$ , denominated in either EJ or dollars) in each year ( $t$ ) using 33 climate models ( $l$ ), two emissions scenarios ( $p$ ) and a resampling of estimates ( $s$ ) that captures uncertainty in the estimation of equation (3). We interpret each of the resulting 33,000 simulation outputs  $D_{t,ps}$  as a potential realization of damages that result from the spatial distribution of warming in model  $l$ , given the overall  $\Delta\text{GMST}$  that is shown by that model under the emissions scenario  $p$ . Multiple simulations lead to an empirically derived distribution of potential outcomes that are conditional on the  $\Delta\text{GMST}$  value for the year, climate model and emissions scenario used to generate that projection. To construct damage functions, we use these outcomes to estimate a conditional distribution of damages<sup>17,18</sup> using ordinary least squares, to obtain expected values, and quantile regressions, to capture uncertainty in damages conditional on  $\Delta\text{GMST}$ .

In our projections of the future, the underlying population distribution and level of per-capita income are evolving over time, thereby shaping the sensitivity of energy consumption to warming and through it, global damages. These changes over time require the construction of year-specific damage functions. Thus, we separately estimate a quadratic damage function in each year:

$$D(\Delta\text{GMST}, t)_{t,ps} = \psi_0^t + \psi_1^t \Delta\text{GMST}_{t,p} + \psi_2^t \Delta\text{GMST}_{t,p}^2 + \varepsilon_{t,ps}, \quad (6)$$

where  $\psi_0^t$ ,  $\psi_1^t$  and  $\psi_2^t$  represent year-specific coefficients to be estimated, and where we use all simulations within a five-year window of year  $t$ , thereby allowing the shape of the function  $D(\Delta\text{GMST}, t)_{t,ps}$  to evolve flexibly and smoothly over the century. Figure 3c shows examples of damage functions at the end of the century, with each point in the scatterplot representing an individual realization of  $D_{t,ps}$ . The left and middle panels demonstrate examples of separate damage functions for electricity and other fuels, respectively, where the realizations are denominated in EJ. In these panels, a realization of  $D_{t,ps}$  is a global aggregation of per-capita consumption impacts projected in every impact region at year  $t$  under climate model  $l$ , emissions scenario  $p$  and simulation  $s$ , that is,  $D_{t,ps} = \sum_j \sum_{r \in j} W_{rjt} \times \text{Impact of climate change per capita}_{c,rjt,l,ps}$ , for fuel category  $c$  (electricity or other fuels), where  $W_{rjt}$  denotes the population of impact region  $r$  in country  $j$  at year  $t$  (Supplementary Section A.3.3). The right panel shows a damage function for total energy expenditure, denominated in dollars. To monetize the projected impacts of climate change on energy consumption, we apply country-specific real prices for electricity and other fuels to the projected quantity impacts, thus reflecting differential costs across geographies and fuels. Hence, a realization of  $D_{t,ps}$  in the right panel is  $\sum_j \sum_{r \in j} \sum_c W_{rjt} \times \rho_{cjt} \times \text{Impact of climate change per capita}_{c,rjt,l,ps}$ , where  $\rho_{cjt}$  denotes a country-year-specific price for fuel category  $c$ . Price trajectories up to 2099 are constructed in one of two ways: (1) by extrapolating present-day prices under various price-growth-scenario assumptions or (2) by utilizing price projections developed in existing IAMs (Supplementary Section C).

In addition to estimating expected damages, we estimate 19 quantile regressions (for every 5th quantile from the 5th to 95th quantiles) to capture the full distribution of damages conditional on  $\Delta\text{GMST}$  (Supplementary Section E.4). Quantile regressions also use a quadratic functional form (equation (6)), but with different coefficients and residuals. The resulting conditional distribution reflects econometric uncertainty in the impact estimates from which damages are constructed, as well as differences in the spatial patterns of warming exhibited across different climate models within the SMME. The 5th–95th quantile ranges from this conditional distribution are indicated by the shaded areas in Fig. 3c.

As described in the next step, we use the estimated dollar-denominated damage functions to compute the net change in global energy expenditures associated with an additional ton of  $\text{CO}_2$ . As

$\text{CO}_2$  is long lived in the atmosphere, the US National Academy of Sciences recommends computing SCC values that capture damages to the year 2300<sup>6</sup>. As CMIP5 models are not run beyond 2099, the SMME sample ends in 2099. Therefore, it is necessary to develop a separate approach to extend these damage functions beyond 2099. Details of this approach can be found in Supplementary Section D.

Figure 3d depicts damage functions for every ten years up to the end of the century (orange and black curves, estimated using equation (6)), as well as extended damage functions for every 50 years post-2100 (grey curves).

## Calculating the partial SCC

In the final step, we combine a probabilistic, simple climate–carbon cycle model with the set of damage functions described above to compute the partial SCC. The partial SCC at time  $t_0$  is defined as the marginal social cost from elevated energy expenditures imposed by the emission of a marginal ton of  $\text{CO}_2$  at  $t_0$  holding all other factors fixed (including the forecast trajectory of baseline greenhouse gas emissions). This is expressed as:

$$\text{Partial SCC}_{t_0} = \sum_{t=t_0}^{2300} DF_t \frac{d\hat{D}(\Delta\text{GMST}, t)}{d\Delta\text{GMST}_t} \frac{d\Delta\text{GMST}_t}{d\text{CO}_{2,t_0}}, \quad (7)$$

where  $\frac{d\Delta\text{GMST}_t}{d\text{CO}_{2,t_0}}$  is the estimated increase in  $\Delta\text{GMST}$  that occurs at each moment in time along the baseline climate trajectory (for example, RCP 8.5) as a result of a marginal unit of emissions at time  $t_0$ , which we approximate with a small pulse of  $\text{CO}_2$  emissions occurring at time  $t_0$ . The values  $\frac{d\hat{D}(\Delta\text{GMST}, t)}{d\Delta\text{GMST}_t}$  are the marginal damages at each moment in time that occur as a result of this small change in future global temperatures; they are computed using the damage functions described in equation (6). The discount factor,  $DF_t$ , converts damages in future year  $t$  into an NPV.

To calculate the change in  $\Delta\text{GMST}_t$  due to a marginal pulse of  $\text{CO}_2$  in 2020, we adapt a version of the FAIR simple climate model that has been developed especially for this type of calculation (Supplementary Section E)<sup>25,70</sup>. Specifically, we use FAIR to calculate  $\Delta\text{GMST}_t$  trajectories for emissions scenarios RCP 4.5 and RCP 8.5, both with and without an exogenous impulse of 1 GtC (equivalent to 3.66 Gt $\text{CO}_2$ ) in the year 2020, an approximation of a marginal emission for which the model numerics are stable. In FAIR, this emissions impulse perturbs the trajectory of atmospheric  $\text{CO}_2$  concentrations and  $\Delta\text{GMST}_t$  for 2020–2300, with dynamics that are influenced by the baseline RCP scenario. In each scenario, the trajectory of damages in the ‘RCP + pulse’ simulation is differenced from the baseline RCP simulation to compute  $\frac{d\hat{D}(\Delta\text{GMST}, t)}{d\Delta\text{GMST}_t} \frac{d\Delta\text{GMST}_t}{d\text{CO}_{2,t_0}}$ , and the resulting damages are converted into US\$ per 1 t $\text{CO}_2$  and discounted to the present.

As there are multiple views on how best to discount future damages (see refs. <sup>6,39,40</sup> for reviews and discussions of various options and their implications), we present multiple estimates using both constant discount rates and ‘Ramsey’ discounting<sup>6</sup>. In the case of a constant discount rate  $r$ ,  $DF_t = e^{-r(t-t_0)}$ . We use the range of values  $r \in \{0.02, 0.025, 0.03, 0.05\}$  to explore the influence of the discount rate. The value  $r = 0.02$  is consistent with ten-year US Treasury rates over the past two decades<sup>71,72</sup> and the remaining values are recommended by ref. <sup>1</sup>.

In the case of Ramsey discounting,  $DF_t = e^{-\sum_{s=t_0}^t r_s I_{s>t_0}}$ , where  $r_s$  denotes the time-varying discount rate for year  $s$ , and  $I_{s>t_0}$  is an indicator variable taking a value of one if year  $s > t_0$ . Time-varying discount rates are calculated according to the Ramsey equation  $r_s = \delta + \eta g_s$ , where the parameter  $\delta$  measures the pure rate of time preference,  $g_s$  measures the growth rate of consumption in year  $s$ , and  $\eta$  is the elasticity of marginal utility of consumption<sup>47</sup>. We use global per-capita income growth from the SSP scenarios to obtain annual values for  $g_s$ , and explore a range of parameter values for  $\delta$  and  $\eta$  based on previous literature<sup>29,39,47,73–79</sup> and guidance from the US National Academy of Sciences<sup>6</sup>.

We present estimates using six combinations of  $\delta$  and  $\eta$  values, choosing from  $\delta \in \{0\%, 1\%\}$  and  $\eta \in \{1, 2, 3\}$ . Details of how these combinations were selected can be found in Supplementary Section E.3.

To capture uncertainty in the climate physics represented in FAIR, we generate a distribution of future temperature trajectories by resampling the equilibrium climate sensitivity, the transient climate response, the short thermal adjustment time and the timescale of rapid carbon uptake by the ocean mixed layer from a joint distribution that we constrain using findings from the literature (Supplementary Section E.2). The solid lines in Fig. 4 indicate the median trajectories when sampling from this constrained joint distribution (Fig. 4b,c) or when sampling jointly from both this conditional joint distribution and quantiles of the damage function (Fig. 4d); shaded areas indicate interquartile ranges. The final range of uncertainty in projected damages (shaded area in Fig. 4d) thus combines uncertainty in climate sensitivity with uncertainty in damages, conditional on the climate sensitivity.

Figure 4e and Extended Data Tables 1 and 2 present partial SCC estimates under RCP 8.5 and RCP 4.5, assuming various discount rates and future energy price scenarios. The 5th–95th percentile ranges (in parentheses) account for econometric and climatological uncertainty (Supplementary Section E.4). Additional partial SCC estimates demonstrating sensitivity to alternative approaches for estimating post-2100 damages, and alternative socioeconomic scenarios can be found in Supplementary Section F.

## Data availability

The data for replicating the findings of this study are available on Zenodo at <https://doi.org/10.5281/zenodo.5099834>.

## Code availability

The code for replicating the findings of this study is available on GitHub at <https://github.com/ClimateImpactLab/energy-code-release-2020/>.

51. Thrasher, B., Maurer, E. P., McKellar, C. & Duffy, P. Technical note: Bias correcting climate model simulated daily temperature extremes with quantile mapping. *Hydroclim. Earth Syst. Sci.* **16**, 3309–3314 (2012).
52. Riahi, K. et al. RCP 8.5—a scenario of comparatively high greenhouse gas emissions. *Climatic Change* **109**, 33–57 (2011).
53. Thomson, A. M. et al. RCP 4.5: a pathway for stabilization of radiative forcing by 2100. *Climatic Change* **109**, 77 (2011).
54. Van Vuuren, D. P. et al. The representative concentration pathways: an overview. *Climatic Change* **109**, 5 (2011).
55. Tebaldi, C. & Knutti, R. The use of the multi-model ensemble in probabilistic climate projections. *Phil. Trans. R. Soc. Lond. A* **365**, 2053–2075 (2007).
56. Riahi, K. et al. The shared socioeconomic pathways and their energy, land use, and greenhouse gas emissions implications: an overview. *Glob. Environ. Change* **42**, 153–168 (2017).
57. Samir, K. & Lutz, W. The human core of the shared socioeconomic pathways: population scenarios by age, sex and level of education for all countries to 2100. *Glob. Environ. Change* **42**, 181–192 (2017).
58. Cuaresma, J. C. Income projections for climate change research: a framework based on human capital dynamics. *Glob. Environ. Change* **42**, 226–236 (2017).
59. Dellink, R., Chateau, J., Lanzi, E. & Magné, B. Long-term economic growth projections in the shared socioeconomic pathways. *Glob. Environ. Change* **42**, 200–214 (2017).
60. IIASA Energy Program SSP Database, Version 1.1 Data set Technical Report (National Bureau of Economic Research, 2016); <https://tntcat.iiasa.ac.at/SspDb>
61. Bright, E. A., Coleman, P. R., Rose, A. N. & Urban, M. L. *LandScan 2011* (2012); <https://web.ornl.gov/sci/landscan/index.shtml>
62. Jiang, L. & O'Neill, B. C. Global urbanization projections for the shared socioeconomic pathways. *Glob. Environ. Change* **42**, 193–199 (2017).
63. Jones, B. & O'Neill, B. C. Spatially explicit global population scenarios consistent with the shared socioeconomic pathways. *Environ. Res. Lett.* **11**, 084003 (2016).
64. Huppmann, D. et al. *IAMC 1.5°C Scenario Explorer and Data hosted by IIASA*. (Integrated Assessment Modeling Consortium & International Institute for Applied Systems Analysis, 2018).
65. Carleton, T. A. & Hsiang, S. M. Social and economic impacts of climate. *Science* **353**, aad9837 (2016).
66. Auffhammer, M. & Aroonruengsawat, A. Simulating the impacts of climate change, prices and population on California's residential electricity consumption. *Climatic Change* **109**, 191–210 (2011).

67. Graff Zivin, J. & Neidell, M. Temperature and the allocation of time: implications for climate change. *J. Labor Econ.* **32**, 1–26 (2014).
68. Schlenker, W. & Roberts, M. J. Nonlinear temperature effects indicate severe damages to US crop yields under climate change. *Proc. Natl Acad. Sci. USA* **106**, 15594–15598 (2009).
69. Wooldridge, J. M. *Econometric Analysis of Cross Section and Panel Data* (MIT Press, 2002).
70. Millar, R. J., Nicholls, Z. R., Friedlingstein, P. & Allen, M. R. A modified impulse-response representation of the global near-surface air temperature and atmospheric concentration response to carbon dioxide emissions. *Atmos. Chem. Phys.* **17**, 7213–7228 (2017).
71. Board of Governors of the US Federal Reserve System 10-year Treasury Inflation-indexed Security, Constant Maturity (DFII10) Technical Report (FRED, Federal Reserve Bank of St. Louis, 2020); <https://fred.stlouisfed.org/series/DFII10>
72. Carleton, T. & Greenstone, M. *Updating the United States Government's Social Cost of Carbon Working Paper* (Univ. Chicago, Becker Friedman Institute for Economics, 2021).
73. Nordhaus, W. *A Question of Balance: Weighing the Options on Global Warming Policies* (Yale Univ. Press, 2014).
74. Arrow, K. J. Global climate change: a challenge to policy. *The Economists' Voice* **4**, 1–5 (2007).
75. Dasgupta, P. The Stern review's economics of climate change. *Natl Inst. Econ. Rev.* **199**, 4–7 (2007).
76. Dasgupta, P. Discounting climate change. *J. Risk Uncertain.* **37**, 141–169 (2008).
77. Hall, R. E. Reconciling cyclical movements in the marginal value of time and the marginal product of labor. *J. Polit. Econ.* **117**, 281–323 (2009).
78. Weitzman, M. L. A review of the Stern review on the economics of climate change. *J. Econ. Lit.* **45**, 703–724 (2007).
79. Weitzman, M. L. On modeling and interpreting the economics of catastrophic climate change. *Rev. Econ. Stat.* **91**, 1–19 (2009).
80. McGrath, G. Natural gas-fired electricity conversion efficiency grows as coal remains stable. *Today in Energy* <https://www.eia.gov/todayinenergy/detail.php?id=32572> (2017).
81. Emission factors for greenhouse gas inventories. US Environmental Protection Agency [https://www.epa.gov/sites/production/files/2018-03/documents/emission-factors\\_mar\\_2018\\_0.pdf](https://www.epa.gov/sites/production/files/2018-03/documents/emission-factors_mar_2018_0.pdf) (2018).
82. IPCC Climate Change 2014: Synthesis Report (eds Core Writing Team, Pachauri, R. K. & Meyer L. A.) (IPCC, 2014).

**Acknowledgements** This project is an output of the Climate Impact Lab consortium that gratefully acknowledges funding from the Carnegie Corporation, Energy Policy Institute of Chicago (EPIC), the International Growth Centre, the National Science Foundation (SES1463644), the Sloan Foundation and the Tata Center for Development. T.C. acknowledges funding from the US Environmental Protection Agency Science To Achieve Results Fellowship (FP91780401). J.R. acknowledges funding from the H2020-MSCA-RISE project GEMCLIME-2020 GA number 681228. We thank L. Alcocer, T. Bearpark, T. Chong, Z. Delgerjargal, G. Dobbels, D. Gergel, R. Goyal, S. Greenhill, I. Higuera-Mendieta, D. Hogan, A. Hussain, T. Kulczycki, R. Li, B. Malevich, M. Norman, O. Nwabuikwu, S. Annan-Phan, C. Schwarz, N. Sharma, J. Simcock, Y. Song, E. Tenezakis, J. Wang and J. Yang for research assistance during all stages of this project, and we thank S. Anderson, J. Chang, M. Landin and T. Mayer for project management. We acknowledge the World Climate Research Programme's Working Group on Coupled Modeling, which is responsible for the CMIP, and we thank the climate modelling groups (listed in Extended Data Fig. 2b) for producing and making available their model output. For CMIP, the US Department of Energy's Program for Climate Model Diagnosis and Intercomparison provides coordinating support and led development of software infrastructure in partnership with the Global Organization for Earth System Science Portals. We thank seminar participants at the UC Berkeley Energy Camp, the University of Chicago EPIC Lunch Series and the Mansueto Institute Lunch Colloquium, LSE Workshop in Environmental Economics, International Energy Workshop, International Workshop on Empirical Methods in Energy Economics, the University of Michigan Sustainability and Development Conference, the Berkeley/Harvard/Yale Environmental and Energy Economics Seminar, the NBER EEE Summer Institute, the UCLA Luskin Center for Innovation Climate Adaptation Research Symposium and the Federal Reserve Bank of Richmond Climate Change Economics Workshop for helpful comments.

**Author contributions** A.R., S.H., M.G., R.K., T.H., A.J., J.R., M.D. and T.C. conceived and planned the study. J.Y., K.E.M., M.D., R.K., A.R., A.J. and T.C. prepared the historical climate data. J.Y., K.E.M., M.D. and R.K. created and prepared the climate projection data. A.R., T.C., A.H., M.D., I.N. and T.H. prepared the energy data. A.R., T.C., A.H., I.N., A.J., J.R., S.H. and M.G. estimated energy-climate response functions. J.R. and A.R. computed projected impacts of future climate change. A.R., M.D., T.C., K.E.M., A.H., I.N., A.J., J.R., S.H. and M.G. constructed damage functions and computed partial social cost of carbon. A.R., S.H. and M.G. wrote the main text, A.R., T.C., A.J., M.D., J.R., J.Y. and K.M. wrote the supplementary materials, and all authors edited.

**Competing interests** A.R., T.C., A.H., A.J., R.K., I.N., J.R. and J.Y. declare no competing interests. M.D., T.H., K.E.M.: The Rhodium Group provides independent research and analysis on a range of global economic topics to clients in the public and private sectors. This includes analysis of global energy market trends. Although some of those clients could potentially be impacted by the results of this research, both positively and negatively, Rhodium staff contributions to this research were conducted completely independently. M.G., S.H. and R.K.: we received no financial or in-kind support for the research conducted in this paper, nor have we received funding or in-kind support from any 'interested' parties. As part of a diversified portfolio, we each hold more than US\$10,000 in stocks and bonds of various companies including those within the energy sector. No other parties have the right to review the paper before its circulation. M.G. holds the position of director at the Energy Policy Institute at the University of Chicago and the Environment and Energy Lab at University of Chicago Labs, and is faculty director at the E2e Lab. From July 2015 to January 2017, M.G. was a member of the US Department of Energy's Secretary

# Article

of Energy Advisory Board. S.H. is the director of the Global Policy Laboratory at the University of California, Berkeley. R.K. previously served as a consultant to Rhodium Group, which provides independent research and analysis on a range of global economic topics to clients in the public and private sectors, including analysis of global energy market trends. R.K. currently serves as director of the Rutgers Institute of Earth, Ocean, and Atmospheric Sciences. R.K. provided technical support to and M.G. was a co-chair of the US Federal Government Interagency Working Group on Social Cost of Carbon between September 2009 and March 2010. R.K. was an author of the National Academies of Sciences, Engineering, and Medicine report *Valuing Climate Damages Updating Estimation of the Social Cost of Carbon Dioxide* published in 2017.

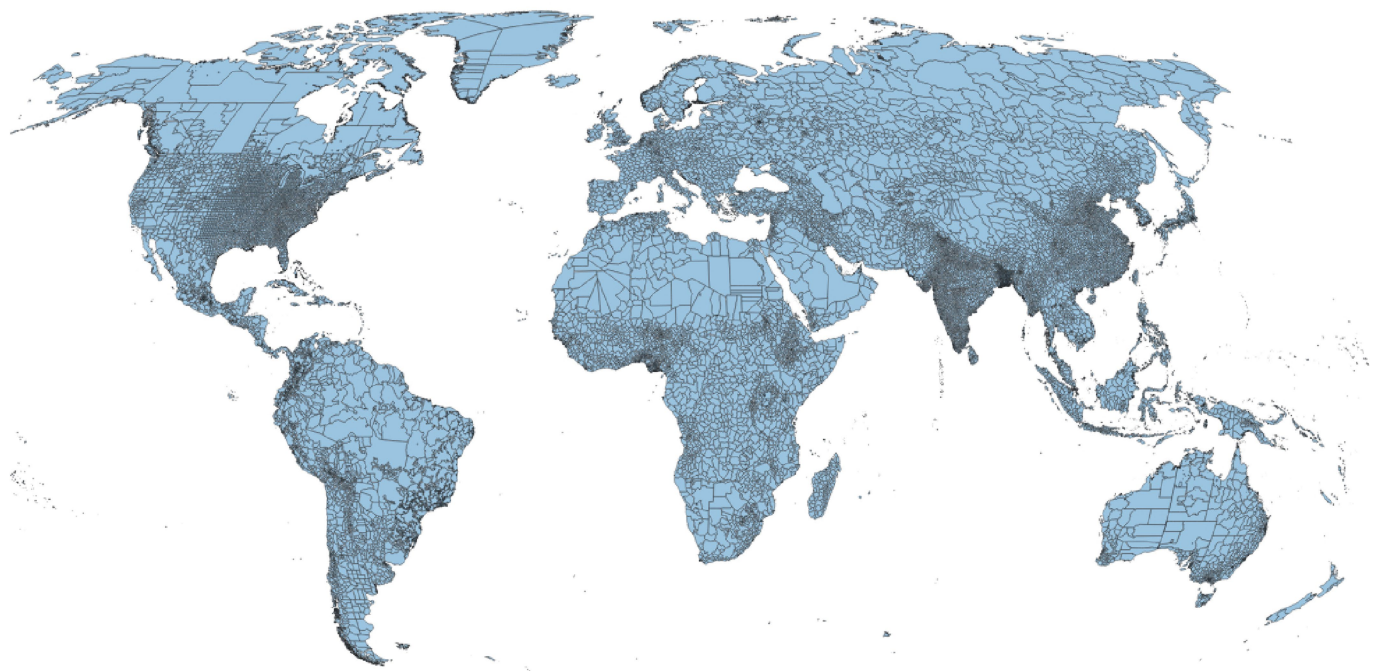
## Additional information

**Supplementary information** The online version contains supplementary material available at <https://doi.org/10.1038/s41586-021-03883-8>.

**Correspondence and requests for materials** should be addressed to Ashwin Rode or Solomon Hsiang.

**Peer review information** *Nature* thanks Katrina Jessie, William Pizer and the other, anonymous, reviewer(s) for their contribution to the peer review of this work. Peer review reports are available.

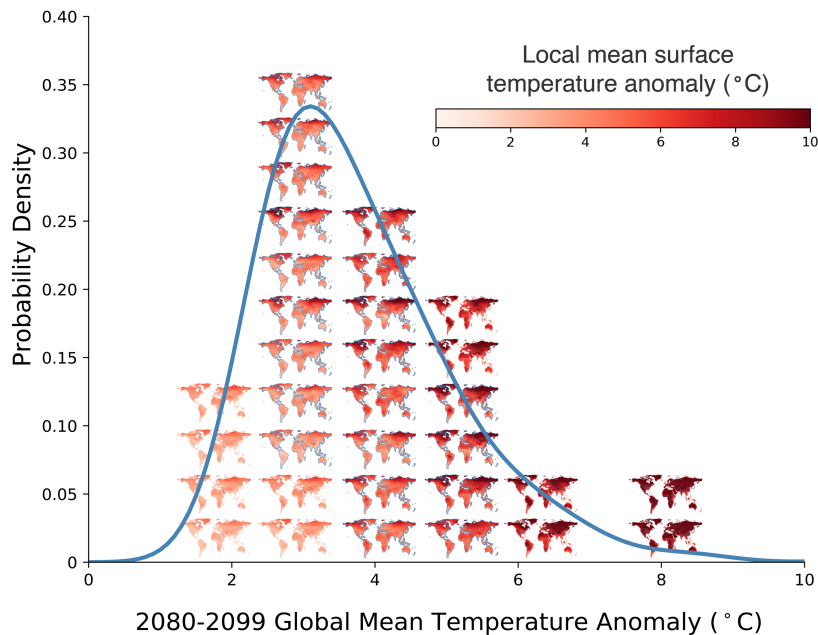
**Reprints and permissions information** is available at <http://www.nature.com/reprints>.



**Extended Data Fig. 1 | Map of the 24,378 “impact regions” for which location-specific projections are calculated.** Map is produced with R software, ggplot2 package, using Global Administrative Region dataset (GADM) basemap<sup>50</sup>. A clustering algorithm<sup>17</sup> is used to form these impact

regions from the full set of GADM administrative regions<sup>50</sup>, such that they are roughly similar in total population, and so that they are approximately internally homogenous with respect to mean temperature, diurnal temperature range, and mean precipitation.

**a Global mean surface temperature anomaly under RCP8.5:  
Distribution across future climate projections**

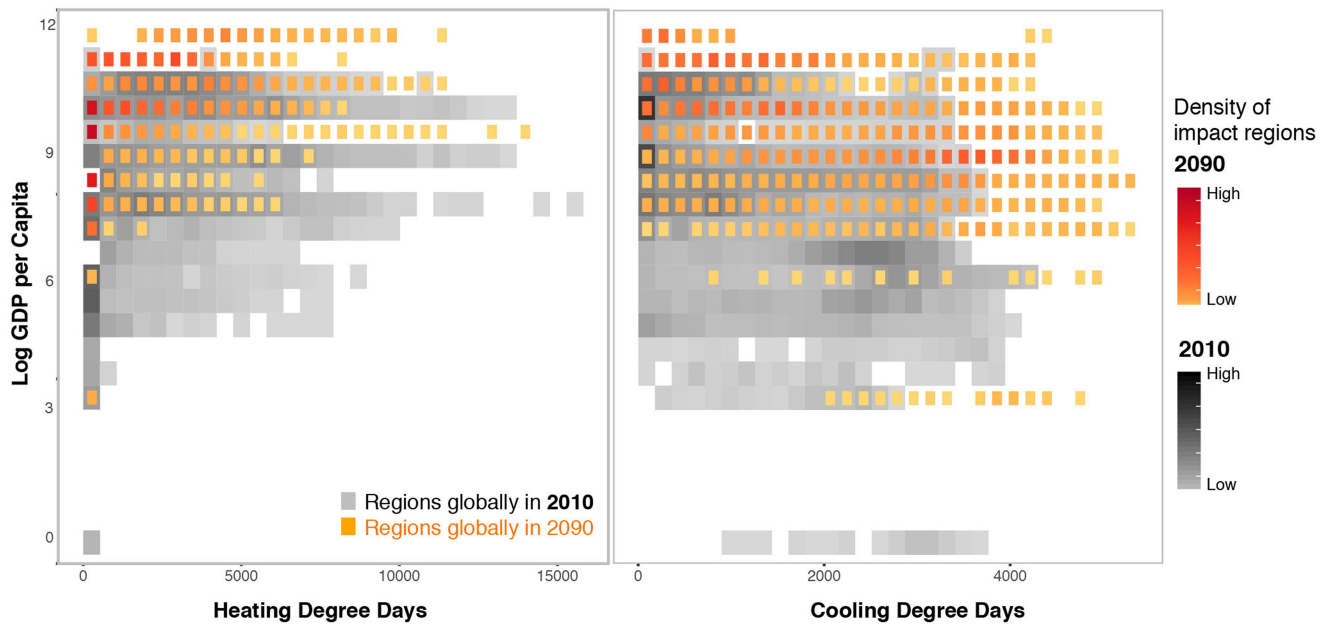


**b Model weights by emissions scenario**

Model or model surrogate name	Weight in RCP4.5	Weight in RCP8.5
ACCESS1-0	3.12%	3.00%
bcc-csm1-1	2.38%	2.29%
BNU-ESM	3.12%	3.00%
CanESM2	3.12%	3.00%
CCSM4	2.38%	2.29%
CESM1-BGC	2.38%	2.29%
CNRM-CM5	2.38%	2.29%
CSIRO-Mk3-6-0	3.12%	3.00%
GFDL-CM3	4.17%	4.00%
GFDL-ESM2G	4.17%	4.00%
GFDL-ESM2M	4.17%	4.00%
inmem4	4.17%	4.00%
IPSL-CM5A-LR	3.12%	3.00%
IPSL-CM5A-MR	3.12%	3.00%
MIROC5	2.38%	2.29%
MIROC-ESM	4.17%	4.00%
MIROC-ESM-CHEM	4.17%	4.00%
MPI-ESM-LR	2.38%	2.29%
MPI-ESM-MR	2.38%	2.29%
MRI-CGCM3	9.37%	9.00%
NorESM1-M	9.37%	9.00%
surrogate.CanESM2.89	1.04%	1.00%
surrogate.CanESM2.94	4.17%	4.00%
surrogate.CanESM2.99	1.04%	1.00%
surrogate.GFDL-CM3.89	1.04%	1.00%
surrogate.GFDL-CM3.94	4.17%	4.00%
surrogate.GFDL-CM3.99	1.04%	1.00%
surrogate.GFDL-ESM2G_01	1.04%	1.00%
surrogate.GFDL-ESM2G_06	-	4.00%
surrogate.GFDL-ESM2G_11	1.04%	1.00%
surrogate.MRI-CGCM3.01	1.04%	1.00%
surrogate.MRI-CGCM3.06	4.17%	4.00%
surrogate.MRI-CGCM3.11	1.04%	1.00%

**Extended Data Fig. 2 | Future climate projections used in generating probabilistic, empirically-based climate change impact projections.** Panel (a) shows local climate distributions under the 21 climate models (outlined maps) and 12 model surrogates (dimmed maps) ('Data assembly' in Methods, Supplementary Sections A.2.2, A.2.3) that are weighted in climate change impact projections so that the weighted distribution of the 2080 to 2099 global mean surface temperature anomaly ( $\Delta\text{GMST}$ ) exhibited by the 33 total models matches the probability distribution of estimated  $\Delta\text{GMST}$  responses

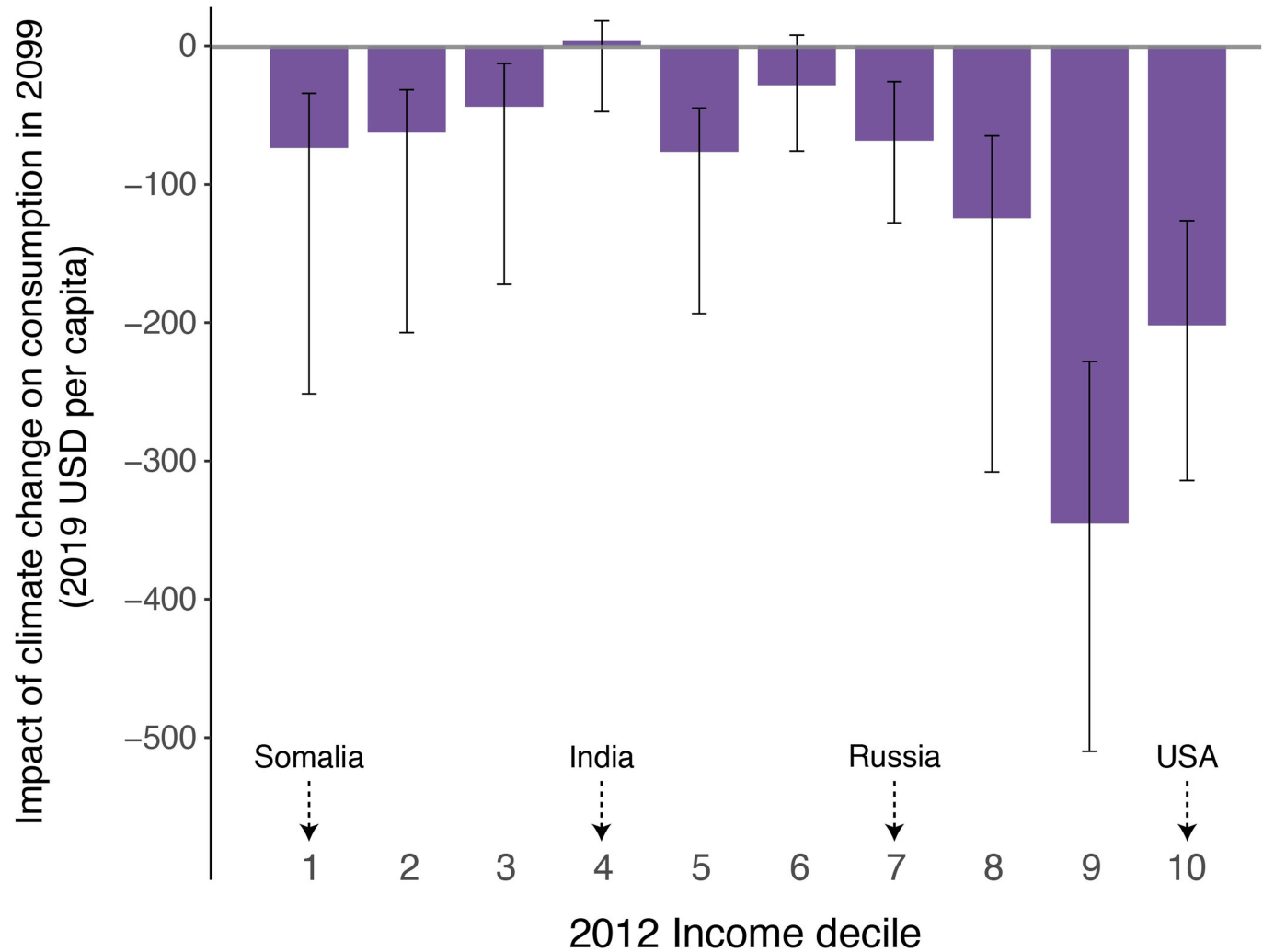
(blue-grey line) under a high (RCP8.5) emissions scenario. For this construction, the anomaly is relative to values in 1986–2005. Maps are produced with Python programming language, using data from ref.<sup>43</sup> and Global Administrative Region dataset (GADM) basemap<sup>79</sup>. Panel (b) lists all 33 models and model surrogates, and their corresponding model weights for both high (RCP8.5) and moderate (RCP4.5) emissions scenarios<sup>43</sup>. These are used to capture climate model uncertainty when generating climate change impact projections under a given emissions scenario (Supplementary Section B.5).



**Extended Data Fig. 3 | Sample overlap between present and future.** The density plots demonstrate the overlap in the joint income  $\times$  long-run climate distributions at 2010 and 2090. Long-run climate is measured by heating degree days (**a**) and cooling degree days (**b**). Distributions are for 24,378 impact regions, in 2010 (grey-black) and 2090 under the RCP8.5 emissions scenario and SSP3 socioeconomic scenario (red-orange). All impact regions within a

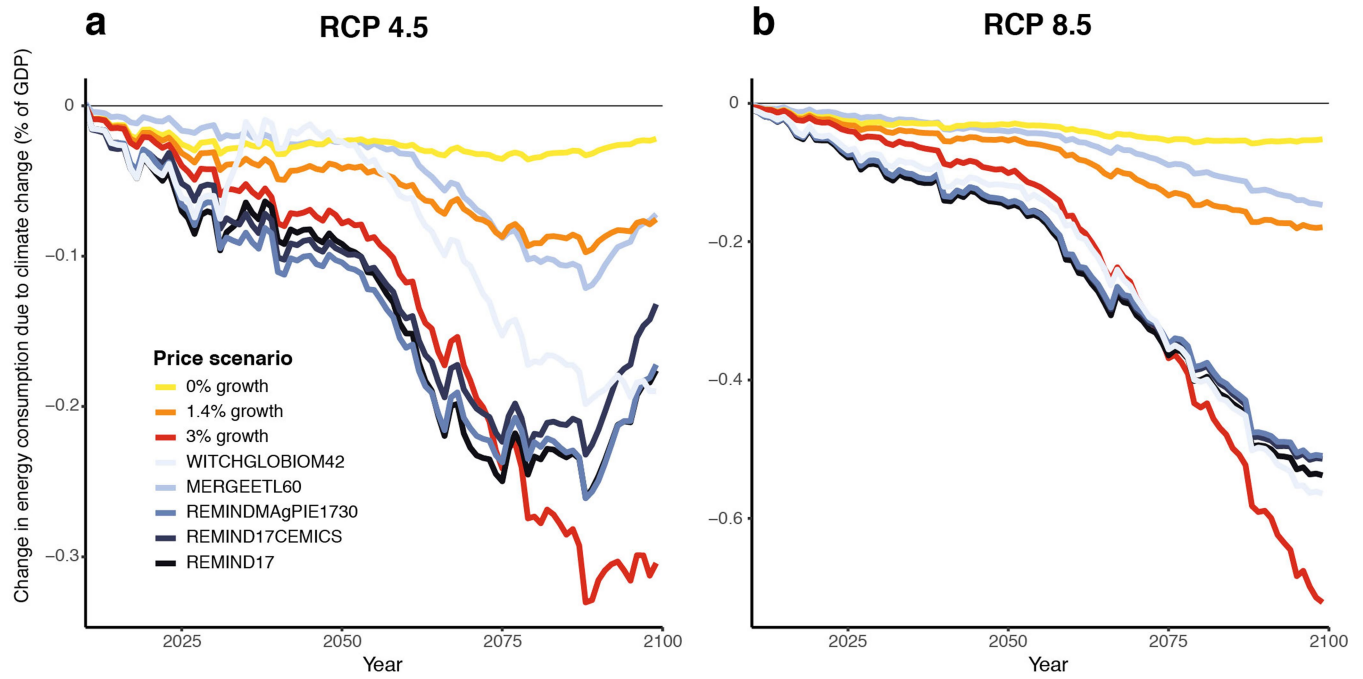
country are assigned the national per capita income. Although the future distribution is shifted towards higher incomes, greater cooling degree days, and fewer heating degree days, the substantial overlap in the two distributions allows for credible extrapolation of energy-temperature responses into the future ('Projecting the impacts of climate change' in Methods).

## Article



**Extended Data Fig. 4 | Climate-change induced changes in total energy expenditures at end-of-century, by present-day income deciles.** The bar chart above depicts annual climate-change induced changes in total energy expenditures at 2099 under a high emissions scenario (RCP8.5) and the SSP3 socioeconomic scenario, separately for each decile of 2012 national per capita income. Income deciles are calculated across all countries at 2012; representative countries in selected deciles are indicated. Expenditures are calculated under a 1.4% annual price growth scenario and are expressed in 2019 USD per capita based on each decile's projected 2099 population. Bars represent mean estimates across an ensemble of 33 climate models. Intervals indicate 5<sup>th</sup>–95<sup>th</sup> percentiles of projected distributions, accounting for climate model and econometric uncertainty (Supplementary Section B.5). The chart demonstrates that heterogeneity in expenditure changes at end-of-century (Fig. 2a) is systematically correlated with present-day national income per capita. Over the upper half of the present-day income distribution, we find that

countries with higher incomes today are generally projected to experience larger overall net savings at end-of-century. This partly reflects the fact that today's richest countries tend to be in temperate climates, where energy savings from fewer cold days will more than offset increases in costs from more hot days. The smallest savings at end-of-century are projected to occur in middle deciles of the present-day income distribution, which is consistent with many of these countries being situated in the tropics and also attaining sufficiently high income levels at end-of-century to increase electricity consumption due to more hot days. The positive correlation between present-day income and net savings at end-of-century does not hold in the lower ranges of today's income distribution. Net savings in today's poorest deciles (i.e. first and second) are actually higher than in the third and fourth deciles, as many of the poorest countries are projected to remain too poor at end-of-century to increase electricity consumption on hot days.

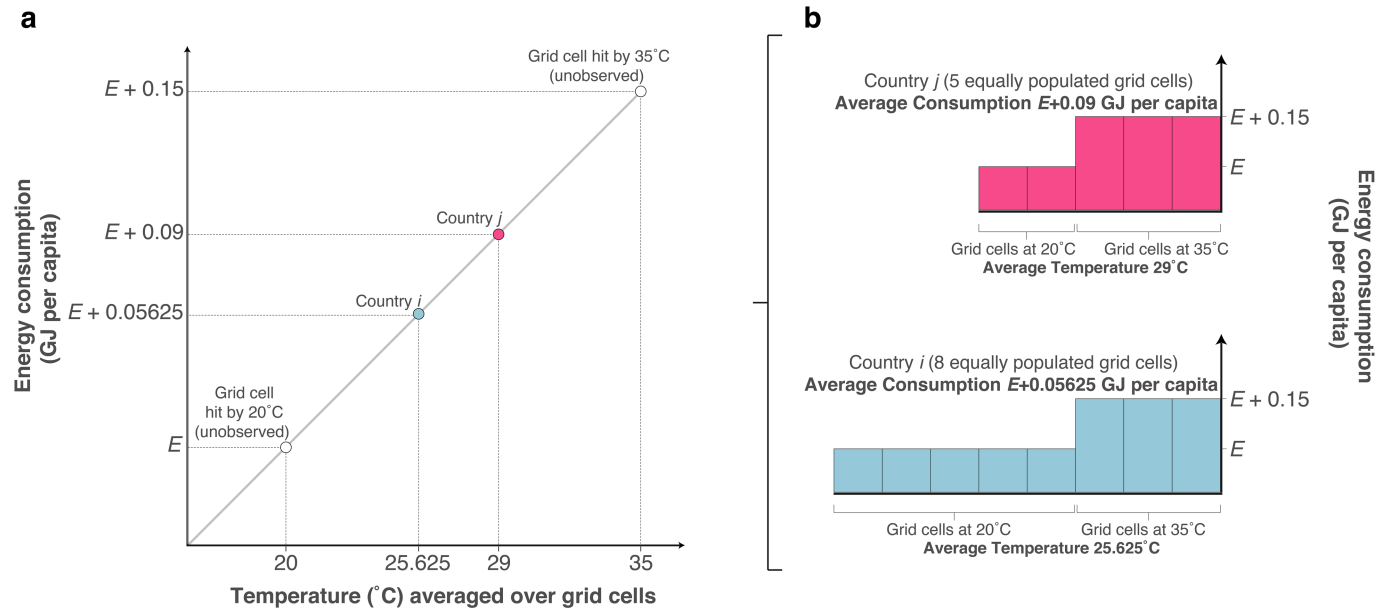


#### Extended Data Fig. 5 | The impacts of climate change on energy

**expenditures.** Time series of changes in total global energy expenditures under the SSP3 socioeconomic scenario for moderate (RCP4.5; Panel **a**) and high (RCP8.5; Panel **b**) emissions scenarios, assuming various energy price trajectories. Three of these trajectories are based on direct extrapolation of present-day price statistics at either moderate (1.4%), stagnant (0%), or high (3%) annual growth rates (Supplementary Section C.1), while five are based on price projections from integrated assessment models (Supplementary

Section C.2) named in the legend. Expenditure changes in a given year are expressed as a percent of global GDP in that year. Aggregate global expenditure changes are obtained by monetizing and summing over the spatially disaggregated impacts across both electricity and other fuels. Regardless of the emissions scenario or assumed price trajectory, end-of-century changes (i.e. net savings) represent a minute fraction of the US \$353 trillion end-of-century global GDP projected under SSP3.

# Article



**Extended Data Fig. 6 | Recovering local temperature-energy consumption relationships using aggregate energy consumption data.** An illustration demonstrating how the effect of local temperature on local per capita energy consumption can be recovered from observations of local temperatures and national per capita energy consumption. **a:** Let a hypothetical, linear response of daily temperature and energy consumption exist at a local (i.e. grid cell) level, depicted by the diagonal grey line. Let  $E$  denote baseline daily energy consumption on a  $20^{\circ}\text{C}$  day. Average per capita energy consumption is observed on day  $d$  in countries  $i$  (blue circle) and  $j$  (pink circle), respectively consisting of 8 and 5 equally populated grid cells experiencing different temperatures. While the temperature is observed in each grid cell, only the national average per capita energy consumption is observed. **b:** Height of each

bar represents unobserved energy consumption on day  $d$  within each grid cell. Pink bars are grid cells in country  $j$  and blue bars are grid cells in country  $i$ . Energy consumption within each grid cell responds to temperature within that grid cell. Averaging temperature and per capita energy consumption across grid cells within each country produces the country-level observations in Panel **a**. A regression using these observations recovers the grid cell-level response. Note that this illustration depicts a linear energy-temperature response for illustrative purposes, however a nonlinear temperature-energy consumption response can be recovered as well, if nonlinear transformations of temperature are computed at the grid-cell-level before being aggregated to the national level ('Econometric estimation of energy-temperature responses' in Methods, Equation 2).

**Extended Data Table 1 | Social cost of energy consumption due to climate change under alternative future price scenarios**

Discount rate:	Constant 2%	Constant 2.5%	Constant 3%	Constant 5%
<b>1.4% price growth</b>				
<b>RCP 8.5</b>	-2.27 (-9.42,0.84)	-1.61 (-5.64,0.24)	-1.25 (-3.70,-0.04)	-0.69 (-1.27,-0.22)
<b>RCP 4.5</b>	-1.73 (-8.49,0.50)	-1.43 (-5.31,0.00)	-1.21 (-3.67,-0.17)	-0.76 (-1.50,-0.27)
<b>0% price growth</b>				
<b>RCP 8.5</b>	-0.99 (-2.97,-0.04)	-0.81 (-1.99,-0.13)	-0.70 (-1.46,-0.17)	-0.47 (-0.72,-0.17)
<b>RCP 4.5</b>	-0.88 (-2.87,-0.11)	-0.81 (-2.08,-0.19)	-0.73 (-1.63,-0.22)	-0.52 (-0.90,-0.20)
<b>3% price growth</b>				
<b>RCP 8.5</b>	-7.45 (-38.77,5.26)	-4.53 (-21.35,2.39)	-3.06 (-12.76,1.04)	-1.20 (-3.04,-0.21)
<b>RCP 4.5</b>	-5.04 (-34.53,3.61)	-3.50 (-19.16,1.36)	-2.63 (-11.68,0.38)	-1.27 (-3.22,-0.33)
<b>MERGE-ETL 6.0 prices</b>				
<b>RCP 8.5</b>	-1.77 (-5.85,-0.34)	-1.18 (-3.36,-0.27)	-0.87 (-2.13,-0.23)	-0.43 (-0.71,-0.14)
<b>RCP 4.5</b>	-1.83 (-6.18,-0.62)	-1.26 (-3.67,-0.43)	-0.95 (-2.43,-0.32)	-0.49 (-0.93,-0.17)
<b>REMIND 1.7 (ADVANCE) prices</b>				
<b>RCP 8.5</b>	-6.40 (-22.19,-1.55)	-4.50 (-13.66,-1.29)	-3.44 (-9.20,-1.10)	-1.80 (-3.38,-0.69)
<b>RCP 4.5</b>	-6.24 (-22.18,-1.88)	-4.58 (-14.00,-1.50)	-3.60 (-9.74,-1.25)	-1.96 (-4.04,-0.75)
<b>REMIND 1.7 (CEMICS) prices</b>				
<b>RCP 8.5</b>	-6.15 (-22.52,-1.45)	-4.32 (-13.73,-1.19)	-3.30 (-9.17,-1.01)	-1.70 (-3.30,-0.63)
<b>RCP 4.5</b>	-6.09 (-21.92,-1.50)	-4.44 (-13.78,-1.28)	-3.47 (-9.55,-1.10)	-1.86 (-3.93,-0.68)
<b>REMIND-MAgPIE 1.7-3.0 prices</b>				
<b>RCP 8.5</b>	-6.04 (-20.53,-1.36)	-4.27 (-12.56,-1.18)	-3.27 (-8.38,-1.03)	-1.72 (-3.00,-0.66)
<b>RCP 4.5</b>	-5.95 (-20.81,-1.80)	-4.39 (-13.09,-1.46)	-3.47 (-9.08,-1.22)	-1.90 (-3.72,-0.73)
<b>WITCH-GLOBIOM 4.2 prices</b>				
<b>RCP 8.5</b>	-6.30 (-23.55,-0.38)	-4.31 (-14.65,-0.49)	-3.22 (-9.88,-0.53)	-1.58 (-3.41,-0.41)
<b>RCP 4.5</b>	-5.58 (-22.81,-0.96)	-4.05 (-14.39,-0.78)	-3.14 (-9.95,-0.66)	-1.65 (-3.95,-0.41)

This table displays estimates of a partial Social Cost of Carbon for excess energy expenditure, under the socioeconomic scenario SSP3. Parentheses contain 5<sup>th</sup>–95<sup>th</sup> percentile ranges, accounting for damage function and climate model uncertainty (Supplementary Section E.4). Costs are valued under various projected energy price trajectories. Three of these trajectories are based on direct extrapolation of present-day price statistics at either moderate (1.4%), stagnant (0%), or high (3%) annual growth rates (Supplementary Section C.1), while five are based on price projections from integrated assessment models (Supplementary Section C.2) named in the table. Costs are discounted to the present using a constant annual discount rate (2%, 2.5%, 3%, or 5%). Estimates using Ramsey discounting are displayed in Extended Data Table 2.

# Article

**Extended Data Table 2 | Social cost of energy consumption due to climate change under alternative future price scenarios**

Discount rate:	Ramsey $\delta = 0\%, \eta = 1$	Ramsey $\delta = 0\%, \eta = 2$	Ramsey $\delta = 0\%, \eta = 3$	Ramsey $\delta = 1\%, \eta = 1$	Ramsey $\delta = 1\%, \eta = 2$	Ramsey $\delta = 1\%, \eta = 3$
<b>1.4% price growth</b>						
<b>RCP 8.5</b>	-13.93 (-81.41,13.56)	-6.00 (-33.28,5.17)	-2.93 (-14.87,2.02)	-3.35 (-16.46,2.13)	-1.90 (-8.20,0.81)	-1.20 (-4.45,0.25)
<b>RCP 4.5</b>	-4.16 (-71.19,14.08)	-2.46 (-28.86,4.99)	-1.60 (-12.93,1.76)	-1.97 (-14.37,1.77)	-1.38 (-7.32,0.54)	-1.01 (-4.11,0.09)
<b>0% price growth</b>						
<b>RCP 8.5</b>	-3.44 (-20.04,2.55)	-1.72 (-8.59,0.87)	-1.00 (-4.10,0.25)	-1.20 (-4.64,0.24)	-0.80 (-2.52,0.00)	-0.58 (-1.51,-0.08)
<b>RCP 4.5</b>	-0.40 (-15.76,2.89)	-0.66 (-6.99,0.89)	-0.63 (-3.53,0.21)	-0.82 (-4.08,0.16)	-0.68 (-2.39,-0.06)	-0.56 (-1.54,-0.12)
<b>3% price growth</b>						
<b>RCP 8.5</b>	-67.08 (-396.41,66.96)	-26.86 (-157.24,25.86)	-11.81 (-67.35,10.56)	-13.03 (-73.36,11.28)	-6.48 (-34.51,4.84)	-3.55 (-17.45,2.11)
<b>RCP 4.5</b>	-29.87 (-374.36,59.47)	-13.14 (-144.86,21.91)	-6.49 (-60.82,8.41)	-7.46 (-65.96,8.78)	-4.21 (-30.71,3.45)	-2.60 (-15.56,1.32)
<b>MERGE-ETL 6.0 prices</b>						
<b>RCP 8.5</b>	-13.02 (-57.46,-1.38)	-5.41 (-22.82,-0.66)	-2.51 (-9.85,-0.36)	-2.82 (-10.77,-0.43)	-1.51 (-5.16,-0.27)	-0.89 (-2.70,-0.19)
<b>RCP 4.5</b>	-12.32 (-60.50,-3.71)	-5.21 (-23.75,-1.64)	-2.47 (-10.20,-0.81)	-2.81 (-11.17,-0.93)	-1.54 (-5.42,-0.52)	-0.94 (-2.90,-0.31)
<b>REMIND 1.7 (ADVANCE) prices</b>						
<b>RCP 8.5</b>	-37.64 (-180.18,-3.60)	-16.55 (-74.59,-2.14)	-8.19 (-33.90,-1.41)	-9.40 (-37.72,-1.74)	-5.34 (-19.21,-1.23)	-3.34 (-10.66,-0.91)
<b>RCP 4.5</b>	-30.56 (-181.99,-5.18)	-14.11 (-74.14,-2.94)	-7.37 (-33.41,-1.82)	-8.61 (-37.22,-2.23)	-5.13 (-19.08,-1.50)	-3.34 (-10.79,-1.06)
<b>REMIND 1.7 (CEMICS) prices</b>						
<b>RCP 8.5</b>	-35.77 (-187.73,-4.09)	-15.79 (-77.19,-2.22)	-7.84 (-34.85,-1.37)	-9.01 (-38.70,-1.68)	-5.13 (-19.55,-1.15)	-3.20 (-10.78,-0.83)
<b>RCP 4.5</b>	-30.33 (-181.98,-0.89)	-13.96 (-73.98,-1.31)	-7.25 (-33.23,-1.14)	-8.46 (-36.97,-1.50)	-5.01 (-18.89,-1.15)	-3.24 (-10.64,-0.87)
<b>REMIND-MAgPIE 1.7-3.0 prices</b>						
<b>RCP 8.5</b>	-35.03 (-168.48,-1.83)	-15.46 (-69.72,-1.38)	-7.68 (-31.61,-1.07)	-8.83 (-35.13,-1.37)	-5.04 (-17.82,-1.06)	-3.16 (-9.85,-0.82)
<b>RCP 4.5</b>	-28.45 (-171.20,-4.30)	-13.22 (-69.76,-2.61)	-6.95 (-31.44,-1.68)	-8.14 (-34.99,-2.08)	-4.88 (-17.92,-1.43)	-3.19 (-10.12,-1.02)
<b>WITCH-GLOBIOM 4.2 prices</b>						
<b>RCP 8.5</b>	-39.88 (-179.02,2.48)	-17.28 (-75.55,0.53)	-8.39 (-34.98,-0.07)	-9.56 (-39.20,-0.17)	-5.30 (-20.27,-0.29)	-3.24 (-11.36,-0.33)
<b>RCP 4.5</b>	-27.64 (-181.90,-2.71)	-12.82 (-74.87,-1.48)	-6.69 (-34.04,-0.94)	-7.79 (-38.04,-1.11)	-4.62 (-19.59,-0.79)	-2.98 (-11.07,-0.59)

This table displays estimates of a partial Social Cost of Carbon for excess energy expenditure, under the socioeconomic scenario SSP3. Parentheses contain 5<sup>th</sup>–95<sup>th</sup> percentile ranges, accounting for damage function and climate model uncertainty (Supplementary Section E.4). Costs are valued under various projected energy price trajectories. Three of these trajectories are based on direct extrapolation of present-day price statistics at either moderate (1.4%), stagnant (0%), or high (3%) annual growth rates (Supplementary Section C.1), while five are based on price projections from integrated assessment models (Supplementary Section C.2) named in the table. Costs are discounted to the present using Ramsey discount rates under various values of the pure rate of time preference,  $\delta$ , and elasticity of marginal utility of consumption,  $\eta$  ('Calculating the partial SCC' in Methods). Estimates using constant annual discount rates are displayed in Extended Data Table 1.

**Extended Data Table 3 | Feedback effects of climate change-induced energy consumption on CO<sub>2</sub> emissions**

	Electricity	Other Fuels
<b>Per capita impact (GJ)</b>	1.2	-2.9
<b>Total impact (billion GJ)</b>	15.0	-36.6
<b>Emissions factor (t CO<sub>2</sub>e per GJ)</b>	0.11	0.05
<b>Additional emissions (Gt CO<sub>2</sub>e)</b>	1.6	-1.8

This table provides a calculation of additional CO<sub>2</sub> emissions in 2099 resulting from projected impacts of climate change on energy consumption under the RCP8.5 emissions scenario and SSP3 socioeconomic scenario. The calculation assumes that all climate change impacts to electricity consumption are powered by a combined cycle natural gas plant with 46% efficiency (i.e. the average 2015 efficiency of US natural gas-fired combined-cycle technology)<sup>80</sup>, and all climate change impacts to other fuels consumption are due to changes in natural gas consumption. Global average per capita impacts at 2099 to electricity and other fuels consumption (Row 1) are taken from projections displayed in Fig. 2c (main text), and are converted to global total impacts (Row 2) by multiplying by the projected world population in 2099 under SSP3. Multiplying total electricity impacts by the emissions factor for natural gas<sup>81</sup> scaled by 46% efficiency, and multiplying total other fuels impacts by the emissions factor for natural gas (Row 3) yields additional emissions from projected climate change-induced electricity and other fuels consumption (Row 4). While assuming all impacts occur through natural gas likely leads to an upper bound in the magnitude of CO<sub>2</sub> emissions feedbacks, the magnitude is nonetheless small when compared to total 2099 global emissions of 100 Gt CO<sub>2</sub> under RCP 8.5<sup>82</sup>. While global CO<sub>2</sub> emissions feedbacks are likely negligible, it is possible that climate change-induced energy consumption will result in substantial changes to local air pollutant emissions in certain locations. The extent of these changes will depend heavily on the shape of the future global energy system, including for example, the location and emissions trajectory of individual electricity generation plants throughout the world and the populations who will be exposed to the air pollution from each. Future research should explore the local air pollution implications of climate change-induced energy consumption.

Reproduced with permission of copyright owner. Further reproduction  
prohibited without permission.